

Re-calibration of SDF/SXDS Photometric Catalogs of Suprime-Cam with SDSS Data Release 8

Masafumi YAGI¹, Nao SUZUKI², Hitomi YAMANOI¹, Hisanori FURUSAWA³, Fumiaki NAKATA⁴, and Yutaka KOMIYAMA¹

¹Optical and Infrared Astronomy Division, National Astronomical Observatory of Japan, Mitaka, Tokyo, 181-8588, Japan
yagi.masafumi@nao.ac.jp

²E.O. Lawrence Berkeley National Lab, 1 Cyclotron Rd., Berkeley, CA, 94720, USA

³Astronomy Data Center, National Astronomical Observatory of Japan, Mitaka, Tokyo, 181-8588, Japan

⁴Subaru Telescope, 650 North A'ohoku Place, Hilo, Hawaii 96720, USA

(Received 2012 August 10; accepted 2012 October 1)

Abstract

We present photometric recalibration of the Subaru Deep Field (SDF) and Subaru/XMM-Newton Deep Survey (SXDS). Recently, Yamanoi et al. (2012) suggested the existence of a discrepancy between the SDF and SXDS catalogs. We have used the Sloan Digital Sky Survey (SDSS) Data Release 8 (DR8) catalog and compared stars in common between SDF/SXDS and SDSS. We confirmed that there exists a 0.12 mag offset in B-band between the SDF and SXDS catalogs. Moreover, we found that significant zero point offsets in i-band (~ 0.10 mag) and z-band (~ 0.14 mag) need to be introduced to the SDF/SXDS catalogs to make it consistent with the SDSS catalog. We report the measured zero point offsets of five filter bands of SDF/SXDS catalogs. We studied the potential cause of these offsets, but the origins are yet to be understood.

1. Introduction

The Subaru Deep Field (SDF; Kashikawa et al. 2004) catalog and the Subaru/XMM-Newton Deep Survey (SXDS; Furusawa et al. 2008) catalog are wide and deep photometric catalogs at high Galactic latitude using the Subaru Prime focus Camera (Suprime-Cam; Miyazaki et al. 2002). They have been used for many studies (e.g., Ouchi et al. 2005; Kashikawa et al. 2006; Hayashi et al. 2007; Furusawa et al. 2011; Toshikawa et al. 2012).

Recently, Yamanoi et al. (2012) identified and reported the discrepancy in B-band and R-band photometry between SDF and SXDS catalogs by comparing them with the Sloan Digital Sky Survey (SDSS) Data Release 8 (DR8; Aihara et al. 2011) photometric catalog¹. The amount of the photometric zero point (ZP) difference is more than 0.1 mag. Kashikawa et al. (2004) wrote that “In any case, the errors in the photometric zero points of our final images would be less than 0.05mag.” and Furusawa et al. (2008) wrote that “... the uncertainties of calibrated photometric zero points of the SXDS images are 0.03 – 0.05 mag rms.” The ZP difference of 0.1 mag is larger than the error that SDF/SXDS claimed.

In this paper, we measure the ZP offset of the SDF and SXDS catalog from SDSS, and investigate the potential causes. It should be noted that the ZP offset also affects the catalog magnitude of extended sources, though we only used photometry of point sources to measure it. The investigation of the possible photometric errors of each object from flat-fielding, sky subtraction, and/or coadding is beyond the scope of this paper, and will be investigated

elsewhere².

The official filter names of the Suprime-Cam, W-J-B, W-J-V, W-C-RC, W-S-I+ and W-S-Z+, are abbreviated as B, V, R, i, and z, respectively. For the difference between the SDSS and Suprime-Cam band, we always subtract Suprime-Cam magnitude from the SDSS one. If we write i-i in a figure, it means i(SDSS)-i(Suprime-Cam). The AB magnitude system (Oke & Gunn 1983) is used throughout the paper.

2. Method

2.1. Problem of the Original Calibration of SDF/SXDS

The original calibration of the SDF and SXDS catalogs was performed in two stages (Kashikawa et al. 2004; Furusawa et al. 2008). First, the photometric result is calibrated using standard stars. The calibration of SXDS depends on the previous work by Ouchi et al. (2001) and Ouchi et al. (2004). Then, a slight ($\simeq 0.05$ mag) shift is applied to the photometric ZP so that the color-color diagram of stars matches the model color-color diagram. The model color is constructed with the atlas of Gunn & Stryker (1983) spectral library(GS83), assuming that the distribution of the color of the stars in GS83 is the same as those in the observed field. SDF used 100 bright $i < 23$ mag stars in the observed field, and SXDS used 700-1100 of $20.5 < R < 23.5$ mag stars.

To verify the assumption that the color of GS83 is the same as the stars in the field, we used another cal-

¹ <http://skyserver.sdss3.org/dr8/en/>

² In this work, we only estimated the total amount of errors, including our color conversion error, in section 3. The total errors are 0.06, 0.02, 0.03, 0.05, and 0.06 mag for B, V, R, i, and z-band, respectively.

ibrated catalog (SDSS DR8). We retrieved stellar objects (type=6 in PHOTOOBJ table in SDSS Catalog Archive Server) in $33.828958 < \alpha(\text{deg}) < 35.158429$, $-5.648833 < \delta(\text{deg}) < -4.354703$ for SXDS and $200.880078 < \alpha(\text{deg}) < 201.444238$, $27.181905 < \delta(\text{deg}) < 27.799080$ for SDF. The areas are 1.714(SXDS) and 0.309(SDF) square degree, and the difference in the area size is the main reason for the difference in the number of the stars. We use psfMag of SDSS hereafter, but our result is the same if we use modelMag instead. SDSS uses asinh magnitude l (Lupton et al. 1999). The Pogson magnitude(Pogson 1856) m is calculated as

$$m = -2.5 \log_{10} [10^{-0.4l} - b^2 10^{0.4l}], \quad (1)$$

where b is a softening parameter. The parameter for each band is given on the SDSS webpage³. In $r < 21$ range, however, the difference between asinh magnitude and Pogson magnitude is negligible (< 0.01 mag) as calculated from equation (1), and we neglect the difference hereafter. The difference between SDSS magnitude and AB magnitude is still under debate. We adopted the offset used in Kcorrect(Blanton & Roweis 2007) $v4^4$; $\Delta m = m_{\text{AB}} - m_{\text{SDSS}} = -0.036, 0.012, 0.010, 0.028, 0.040$ in u, g, r, i, and z bands. Though the precision of the values is not explicitly given, we expect that it would be smaller than 0.01 mag, since the values have a 0.001 digit. In SDSS-DR8, some stars have multiple entries in the database, as they were observed more than once. We calculate the magnitude difference in g,r,i and z-band between each pair of the entries of stars observed multiple times. We adopted a threshold of difference as 3σ ($3 \times \sqrt{\text{psfMag_Err}_1^2 + \text{psfMag_Err}_2^2}$), and if the difference is larger than the threshold, the star is not used in our analysis, since it might be a variable star. If the difference is smaller than the threshold, the psfMag of the multiple entries are averaged and used in the following analysis.

The synthetic color of GS83 stars are calculated following the equation (9) of Fukugita et al. (1995) using the transmission by Doi et al. (2010), and overlaid on the catalog colors of SDSS stars in figure 1. Doi et al. (2010) measured the responses of correctors, filters and CCDs in SDSS using a monochromatic illumination system. Then it is multiplied with the model reflectivity of the primary and the secondary mirrors and given in their Table 4. We multiplied it with the atmospheric transmission at 1.3 air-mass given in the table, and the product was used as the SDSS transmission in this study. Doi et al. (2010) reported that the variation of the response function may amount to 0.01 mag in g,r,i and z band, but it is cancelled by a calibration procedure, and does not appear in the final SDSS catalogs. They concluded that the residual effects are smaller than 0.01 mag for all passbands. We can therefore expect that the error of synthetic magnitudes due to a possible error of the transmission curve would be < 0.01 mag.

Since the GS83 spectral energy distribution (SED)

adopts the air wavelength while SDSS transmission uses the vacuum wavelength, we converted the SED to the vacuum wavelength using the index of Ciddor (1996), which has very small ($< 0.1\%$) difference from the IAU standard by Morton (1991). We omitted 22 stars from the plot since they lack data at some wavelength within g, r, and/or i passband.

In figure 1, it is clearly seen that GS83 stars have an offset from SDSS stars to the right-bottom direction. The possible effect of the Galactic extinction is checked with the extinction curve by Cardelli et al. (1989) and O'Donnell (1994) with $R_v=3.1$. The reddening vector is also written in figure 1. As the reddening is a bit different in different SED, we plotted the median reddening vectors for O, and M-type stars in GS83. The direction of the GS83 offset from SDSS stars is perpendicular to the reddening, and therefore the offset is not caused by the Galactic extinction.

We calculate the amount of the offset by comparing the distribution of GS83 stars with an empirical fit of the distribution of SDSS stars. Jurić et al. (2008) gives an analytical expression of (g-r) color of SDSS stars as a function of their (r-i) color. The amount of (g-r) offset of GS83 stars from the fit is shown in figure 2. The median offset of (g-r) is 0.13 mag for the $-0.2 < (r-i) < 0.7$ clump.

This color offset between SDSS and GS83 was already recognized by previous studies (e.g., Lenz et al. 1998; Fukugita et al. 2011). Fukugita et al. (2011) discussed that the offset is explained by the metallicity variance. They investigated the color of stars in the SDSS system using a photometric catalog of SDSS-DR6(Adelman-McCarthy et al. 2008). The blue GS83 stars are metal-rich disk stars, while the SDSS stars, especially at high Galactic latitude, are metal-poor popII stars. We discuss the metallicity effect in section 4.2.1. Here we stress that the color distribution of GS83 stars would not be a good representation of that of the faint field stars that were used for the SDF/SXDS calibration.

2.2. Color Conversion from SDSS to Suprime-Cam System

In this study, we return to a classical color calibration method; a color conversion between filter systems. If we can convert the SDSS catalog magnitude to the AB magnitude in the Suprime-Cam system, all the stars in SDSS would be used as photometric standards. Though the photometric error of SDSS (~ 0.04 mag) is relatively larger than that of the well-calibrated photometric standard stars (e.g., < 0.01 mag; Landolt 2009), or that of the spectrophotometric standard stars (e.g., $< 0.5\% \sim 0.005$ mag ; Bohlin et al. 2010) the large number of SDSS stars, > 50 stars in a Suprime-Cam field will make the systematic error smaller. This method was not possible when the SDF or SXDS catalog was constructed, since the SDSS catalog of the region did not exist. Now this method is promising, thanks to the wide coverage of the SDSS DR8 catalog. We fit the difference of Suprime-Cam magnitude and SDSS magnitude as a function of the SDSS color;

³ <http://www.sdss3.org/dr8/algorithms/magnitudes.php#asinh>

⁴ <http://howdy.physics.nyu.edu/index.php/Kcorrect>

$$SDSS - Suprime = c_0 + c_1(color) + c_2(color)^2 + \dots \quad (2)$$

2.2.1. Model SEDs

In our previous work (Yagi et al. 2010), we fit Bruzual-Persson-Gunn-Stryker atlas (BPGS)⁵⁶ colors with quadratic functions. BPGS is an extrapolation of the original GS83 data, and is also used in this study instead of GS83, hereafter. In this work, we first use the model spectral energy distributions (SEDs) to cover a wider variation of stars, such as low-metal stars. We retrieved several flux calculation of ATLAS9 models (Castelli & Kurucz 2004) on the web (ATLAS9 grids)⁷. The input parameters are the metallicity ([Fe/H]), the alpha enhancement ([α /Fe]), the temperature (T), the surface gravity (log g), mixing length parameter (l/H), the Helium enhancement (DY), and the perturbation velocity (v_{turb}). We adopted $l/H=1.25$, $v_{\text{turb}}=2\text{km s}^{-2}$, and $DY=0$ models, because these parameters are used as default values in the ATLAS9 grids. The temperature range is $3750\text{K} \leq T \leq 50000\text{K}$. Since the relation between the temperature and the surface gravity changes according to [Fe/H], the possible combinations are taken from Yonsei-Yale(Y²) isochrone version 2 (Yi et al. 2001; Demarque et al. 2004), which covers $0.4 < M_{\text{initial}}/M_{\odot} < 5$ stars. In the isochrone, stars of all ages are used. We used [α /Fe]=0.3 models in Y² for [α /Fe]=0.4 models to set constraints on the combinations of [Fe/H], T and log g. Note that low mass ($M_{\text{initial}}/M_{\odot} < 0.4$) stars, subdwarfs and white dwarfs are not included in the model.

The set of [Fe/H] and [α /Fe] we used are (+0.5,0.0), (+0.5,+0.4), (0.0,0.0), (0.0,+0.4), (-0.5,0.0), (-1.5,0.0), (-1.5,+0.4), and (-2.5,+0.4). The set of the temperature and surface gravity are taken from Y² isochrone (Yi et al. 2001; Demarque et al. 2004). We do not apply Galactic extinction at this stage. The effect of the Galactic extinction is investigated later.

2.2.2. System Responses

For SDSS synthetic magnitude, we adopted the transmission by Doi et al. (2010). It includes the atmospheric effect at airmass=1.3 at the SDSS site. The Suprime-Cam response is calculated as the product of the quantum efficiency(QE) of MIT/Lincoln Laboratory (MIT/LL) CCDs⁸, the filter responses⁹, the transmittance of the primary focus corrector¹⁰, and the reflectivity of Primary mirror¹¹. The extinction of a model atmosphere at airmass=1 is then multiplied. The total throughput curves are slightly different from the one used in SDF and SXDS photometric calibrations, because of the update of the responses of the telescopes, and difference of the airmass. However, the difference is negligible (<0.01mag) in this study. It should also be noted that the SDSS system is at airmass=1.3, and Suprime-Cam system is at airmass=1. The possible effect of the change in airmass

on the Suprime-Cam system is investigated later.

The synthetic AB magnitude is calculated by multiplying the model SEDs and the system response. The wavelength of model SEDs by ATLAS9 are in a vacuum, and the Suprime-Cam response is in the air. We corrected the SED to the air wavelength and measured the color. Note that the difference of the wavelength between in the vacuum and in the air is $1 - 2\text{\AA}$, and makes 0.007 mag difference at most.

2.2.3. Conversion Function

We then fit the equation (2) to the model color distribution. The internal calibration error of SDSS DR8 is claimed to be 0.01 mag in g,r,i, and z-band (Aihara et al. 2011). DR8 adopted uercal method (Padmanabhan et al. 2008), and the absolute zero point is calibrated against DR7 (Abazajian et al. 2009). The absolute zero point error of DR6 is evaluated by Fukugita et al. (2011). They compared photometry against spectroscopic data, and concluded that the error is smaller than 0.04 mag. Since the data handling of DR7 is the same as DR6, the error of the absolute calibration of DR7 and DR8 would be smaller than 0.04 mag. We therefore aim to obtain a fit whose systematic error $\lesssim 0.04$ mag. The order of the polynomial is set so that Akaike's Information Criterion is minimal. The fit results are shown as figure 3, and the coefficients are presented in table 2. In the color range shown in the table, the deviation of the model color from the fitting polynomial is smaller than 0.04 mag.

2.3. Application to the Empirical SEDs

We collected four empirical SEDs; BPGS, HILIB(Pickles 1998), STELIB(Le Borgne et al. 2003), and The Indo-U.S. Library of Coudé Feed Stellar Spectra (CFLIB; Valdes et al. 2004) to see whether the color conversions also work well for them. We did not interpolate the SEDs, and the data which lacks some part in the filter coverage were omitted. The result is shown in bottom panels of figure 3. Most of the color deviations are within the $-0.04 < \Delta < 0.04$ range, except for a few ($\sim 1\%$ in B, at most) outliers.

2.4. The Effect of Galactic Extinction

The color of the stars is changed by the Galactic extinction, and we can only know the upper limit of the extinction. We adopted the model first developed by Cardelli et al. (1989) and updated by O'Donnell (1994), and applied an $A_v=1$ extinction with $R_v=3.1$ to the model SEDs to see how the deviation changes. The reddened SDSS color versus residual is plotted in figure 4. Because of the nonlinear fit of the equation (2), the nearly linear shift of the distribution by Galactic extinction makes the distribution winding. Even with the extreme $A_v=1$ reddening, however, the fit is better than ± 0.04 mag in the selected color range. For the SDF and SXDS field, the total Galactic extinction is $A_v=0.049$ and 0.058 , respectively, from Schlafly & Finkbeiner (2011) via NASA/IPAC Extragalactic Database(NED)¹². We can therefore expect

⁵ <http://www.stsci.edu/hst/observatory/cdbs/bpgs.html>

⁶ <ftp://ftp.stsci.edu/cdbs/grid/bpgs/>

⁷ <http://www.user.oat.ts.astro.it/castelli/grids.html>

⁸ http://www.naoj.org/Observing/Instruments/SCam/ccd_mit.html

⁹ <http://www.naoj.org/Observing/Instruments/SCam/sensitivity.html>

¹⁰ <http://www.naoj.org/Observing/Telescope/Parameters/PFU/>

¹¹ <http://www.naoj.org/Observing/Telescope/Parameters/Reflectivity/>

¹² <http://ned.ipac.caltech.edu/forms/calculator.html>

that the effect of Galactic extinction on SDF and SXDS catalogs does not affect the color conversion much.

2.5. The Effect of Atmospheric Extinction

The atmospheric extinction is another factor to change the color conversion. The SDF and SXDS were observed in various airmasses. We estimated the exposure time weighted mean of the airmass using the Subaru STARS archive (Takata et al. 2000). The result is shown in table 3. The mean airmass is between 1. and 1.6. We can also see a trend that longer wavelength data are observed in larger airmass. Observers know that seeing size in shorter wavelength is likely to be affected by the airmass, while lights of longer wavelength are less dimmed by atmospheric extinction, observers prefer to observe shorter wavelength at smaller airmass. This may introduce some systematic biases in the calibration.

We used an atmospheric extinction curve shown in figure 5. The model is constructed using the high resolution line extinction data by Stevenson (1994) and the Mauna Kea extinction model. The change of the SDSS color vs Δ color relation is shown in figure 6. We fit a function

$$\Delta m = k_1 \times (\text{airmass}) + k_2 \times (\text{airmass}) \times (\text{color}) \quad (3)$$

to the difference of the synthetic magnitude between airmass=1 and 2 models. The coefficients are shown in table 4. In figure 6, only $k_1(\text{airmass} - 1)$ is corrected. After the correction of the linear airmass term, we cannot see any difference among the different airmass models in V, R, and i-band relations, as suggested by small k_2 . In B-band, a (g-r)=1.5 object would brighter by ~ 0.02 mag at airmass=2. In z-band, an (i-z)=1.5 object would brighter by ~ 0.01 mag at airmass=2. It should be noted that the extinction in magnitude is not a linear function of the airmass when a cross-term of color and airmass exists, and it makes the airmass=3 model in z-band slightly shifted.

In airmass<3, the relations are in the ± 0.04 mag range. If we use this SDSS color versus (SDSS)-(Suprime-Cam) plot, the airmass effect is small, and the difference of the mean airmass among the different bands would have no effect.

2.6. The Effect of Recession Velocity

The model spectra are calculated in the rest frame. The recession velocity of a star makes the spectrum redshifted/blueshifted, and may change the color. In faint magnitude, the majority of stars will be halo stars, and they would have a large recession velocity in some field, because of the rotation of the sun around the Galaxy. We constructed ± 300 km s⁻¹ model spectra and made SDSS color vs Δ color plots. The result is shown in figure 7. In z-band calibration, we can see a slight offset, but the difference is 0.006 mag at most. We can conclude that the effect of the recession velocity on the color conversion is negligible for Galactic stars.

3. Result

We then re-calibrate the ZP of SDF and SXDS catalogs using the color conversion in the previous section. We used the public catalog of SDF Data Products version 1¹³ and SXDS Data Release 1 (DR1)¹⁴. SXDS consists of 5 fields, SXDS-C, SXDS-N, SXDS-S, SXDS-E, and SXDS-W, which are defined in Furusawa et al. (2008). Both catalogs used Suprime-Cam (Miyazaki et al. 2002) with MIT/LL CCDs. The MAG_AUTO parameter is used for the magnitude. The Galactic extinction is not corrected in the catalog. We set constraints so that FWHM is smaller than 8 pixels (1.6arcsec), and brighter than 24 mag. For both catalogs, all combinations of the detection band and the measurement band are available, but we used catalogs whose detection band is the same as the measurement band.

We cross-matched the SDF and SXDS catalogs with stars in SDSS DR8. The object within 2 arcsec from the SDSS star is regarded as the corresponding object. We first select the nearest SDSS star within 2 arcsec from each SDF/SXDS star. If an SDSS star is assigned to more than one SDF/SXDS star, the nearest pair is kept for identification.

The residual of coordinates of stars in r-band magnitude of $20 < r < 21$ are shown in figure 8, where we simply converted $\xi = \alpha \cos(\delta)$ and $\eta = \delta$. Though the astrometry of SXDS-C shows a larger scatter, the radius of 2 arcsec of cross-match covers the difference.

The SDSS magnitude versus the difference color of the SDSS and Suprime-Cam is shown as figure 9. In the figure, the object whose Suprime-Cam magnitude is fainter has a negative difference in y. The tendency that bright objects has a negative difference is due to a saturation in Suprime-Cam data. As it is not simple to exclude saturated objects from the catalog correctly, we did not apply any selection of saturation in this study. Note that the difference in y is not corrected for the color dependence, and therefore the relation is broad. For example, the two loci in V-band correspond to two different populations, distant blue stars and closer red stars.

From figure 9, we adopted the magnitude range for the calibration; $20.5 < g < 21.5$ for B and V, $20 < r < 21$ for R, $19.5 < i < 20.5$ for i, and $19 < z < 20$ for z. In the magnitude range, the saturation of Suprime-Cam stars has no effect. We also set a constraint that the error of the SDSS photometry, $\text{psfMag_Err} < 0.1$, to avoid poor photometry data. Then, the SDSS color versus the difference color of the SDSS and Suprime-Cam in the magnitude range are plotted in figure 10. They correspond to the top panels of figure 3. In some panels, we can see a significant offset from the model color distribution. The green filled circles with errorbars show the median of the (SDSS)-(Suprime-Cam) color in 0.2 mag bin of SDSS color. The errorbar represents the root mean square (rms) of the bin estimated from the median of the absolute deviation (MAD) as

¹³ <http://soaps.nao.ac.jp/SDF/v1/index.html>

¹⁴ http://soaps.nao.ac.jp/SXDS/Public/DR1/index_dr1.html

$$\text{rms} = \text{MAD} \times 1.4826. \quad (4)$$

The trend is almost parallel to the distribution of the model distribution. The apparent difference in the slope between the model and the catalog in z-band is a fake. It was made by the relatively larger dispersion of z(SDSS) (~ 0.07 mag) compared with that of i(SDSS) (~ 0.04 mag) and z(Suprime-Cam) (< 0.01 mag). The distribution is elongated from top-left to bottom-right by the error of z(SDSS), and taking a median of z(SDSS)-z(Suprime-Cam) after binning in i(SDSS)-z(SDSS) changed the apparent slope. If we plot i(SDSS)-z(Suprime-Cam) vs z(SDSS)-z(Suprime-Cam), the z(SDSS) error is perpendicular to the binning axis, and the model and the catalog is almost parallel. The result suggests that the difference between the SDSS and Suprime-Cam catalog would be the offset of the ZP of Suprime-Cam catalogs.

We then estimate the offset of the ZP of the SDF and SXDS catalogs from the SDSS based on an estimation using the parameters in table 2. The number of stars, the median of the offset, and the rms of the distribution (σ) calculated from the MAD are shown in table 5. The offset is also plotted as a function of the wavelength as figure 11, where open squares represent SDF, and other symbols represent SXDS fields. For SXDS, a clear correlation between the wavelength and the offset is recognized.

In table 5, the σ (5th column) is the rms of the distribution and not the error. The determination error of the offset from statistics is roughly approximated by $\sigma\sqrt{\pi/2N} \sim 0.01$ mag, where $\sqrt{\pi/2}$ is the factor for the rms of the median. The σ mainly comes from the photometric error of SDSS. We calculated the contribution of the SDSS error as

$$\sigma_{\text{SDSS}} = \text{median}(\text{psfMag_Err}), \quad (5)$$

and is shown in the 6th column in table 5.

The σ is partly explained by the SDSS error. If we subtract the effect, the mean residuals of the 6 fields are 0.06, 0.02, 0.03, 0.05, and 0.06 mag for B, V, R, i, and z-band, respectively. The residuals include the intrinsic dispersion around our best fit, which is the error of our color conversion, and the error of the data reduction and the photometry.

Some Suprime-Cam data show an offset even larger than the sigma of the distribution, and the offset is significant. These values are shown in bold in table 5. In B-band, the offset is different between SDF and SXDS by 0.13 ± 0.01 . On the other hand, no difference is seen among the fields in V-band and R-band. The systematic difference between SDF and SXDS seems to be marginal in z-band, 0.07 ± 0.01 . In i-band, the variation of the estimated offset is large (peak-to-peak 0.06 mag).

In summary, we found a significant offset of ZP in some of the SDF/SXDS catalogs at bright ($r \sim 20$) magnitude stars from AB magnitude of SDSS. The amount of the offset is significantly larger than the estimated uncertainty from the catalogs. If we correct the ZP offset, the distribution of the (SDSS)-(Suprime-Cam) color follows the model sequence well. Examples are shown as figure 12.

4. Discussion

4.1. The Color Histogram of Faint Objects in SDF and SXDS

The different offset of B-band and z-band (figure 11) makes the color distribution of SDF and SXDS different. We made a color histogram of faint objects in SDF and SXDS-C and compared them. Most of the faint objects are galaxies. We used the R-band selected catalog, the R-band based object extraction and MAG_AUTO.

For the B-band check, we used (B-R) color, because Yamanoi et al. (2012) calibrated and checked B and R-bands. The Galactic extinction is assumed to be $(A_B, A_R) = (0.07, 0.04)$ for SDF¹⁵, and $(0.091, 0.056)$ for SXDS-C (Furusawa et al. 2008). The result is shown as the left panel of figure 13. The slight difference in the size of the observed area is not corrected. In the original catalogs, the blue end of the color histogram is different (figure 13 top-left). The difference gets smaller if we use our re-calibrated catalogs (figure 13 bottom-left).

The (i-z) color histogram is shown as the right panel of figure 13. The Galactic extinction is $(A_i, A_z) = (0.03, 0.02)$, and $(A_i, A_z) = (0.044, 0.031)$ for SDF and SXDS-C, respectively. Our correction again decreases the apparent difference of the color distribution.

This result suggests that the different ZP offset between SDF and SXDS in B-band and z-band would be due to a calibration error, and not coming from possible inhomogeneity of SDSS DR8. The result also shows that the offset of magnitude found around $R \sim 20$ mag stars would be similar in $R \sim 24$ mag objects. It supports our assumption that the difference between the SDSS-based magnitude and the original SDF/SXDS magnitude would be an offset of the ZP in SDF/SXDS catalogs.

4.2. Possible Origins of the ZP Offset

4.2.1. Metallicity Effect on the Color-color Diagram

In figure 14, we plotted BPGS stars and ATLAS9 models. We plotted model points with $[\text{Fe}/\text{H}] = 0$ and $[\alpha/\text{Fe}] = 0$ (hereafter $[\text{Fe}/\text{H}] = 0$ model) as filled green circles and those with $[\text{Fe}/\text{H}] = -2.5$ and $[\alpha/\text{Fe}] = 0.4$ (hereafter $[\text{Fe}/\text{H}] = -2.5\text{a}$ model) as filled red circles. The $[\text{Fe}/\text{H}] = 0$ model seems suitable in all the color combinations in ATLAS9. For a comparison, we plotted SDSS stars of ($15 < r < 21$) in SDF and overlaid models in figure 15. The $[\text{Fe}/\text{H}] = -2.5\text{a}$ models well covers the SDSS color distribution on the bluer side, and $[\text{Fe}/\text{H}] = 0$ model is somewhat better on the redder side.

The reason why the color-color diagram (figure 15) shows the offset between different metallicities but not in figure 3 is simply the difference in the central wavelength of the filters used in the y-axis. The variation of slope and curvature of the spectrum has less of an effect on the y-axis for a pair of passbands which have close central wavelengths.

The trend that blue stars are metal poor is understood by the color-magnitude relation of the stars, and the

¹⁵ http://soaps.nao.ac.jp/SDF/v1/common/galactic_extinction

metallicity gradient along the distance from the Galactic disk. We checked this effect using a simple model. We adopted a metallicity distribution by Peng, Du, & Wu (2012), and connected them with intercepts as

$$\begin{aligned} [\text{Fe}/\text{H}] &= -0.21|z| \quad (|z| < 2) \\ &-0.16|z| - 0.1 \quad (2 \leq |z| < 5) \\ &-0.05|z| - 0.65 \quad (5 \leq |z| < 48) \\ &-3 \quad (48 \leq |z|), \end{aligned} \quad (6)$$

where z is the distance from the Galactic plane in kilo parsec unit. Then the correlation of the color and the metallicity is calculated for a certain apparent magnitude. We used the color and the magnitude from Y^2 isochrone with Green et al. (1987) color models (Yi et al. 2001; Demarque et al. 2004), as the model SEDs do not give the radius of the star, and therefore the calculation of the absolute magnitude is difficult to perform. We adopted $[\alpha/\text{Fe}]=0.3$ for $[\text{Fe}/\text{H}] \leq -1$, and $[\alpha/\text{Fe}]=0$ for $[\text{Fe}/\text{H}] > 1$. Note that the Y^2 model prepares $[\alpha/\text{Fe}]=0.3$ and 0.6 , while the ATLAS9 grids prepare $[\alpha/\text{Fe}]=0.4$. Then, the metallicity, the color and the absolute magnitude are obtained from the isochrone. When we set an apparent magnitude, the absolute magnitude is converted to the distance, and then it is converted to z using the Galactic latitude. If the metallicity is within ± 0.1 of equation (6), the point is plotted. In figure 16, we plotted the (B-V) color versus metallicity relation of $V=14$ and $V=19$ magnitude stars in Galactic latitude of 60 and 80 degree fields, which correspond to SXDS and SDF fields. Note that the color of Green et al. (1987) is in the Johnson UBV system, and $(B-V)_{\text{AB}}=(B-V)_{\text{Vega}}+0.10$ (Fukugita et al. 1995). We corrected the color for the magnitude system difference in figure 16. The trend is thus reproduced by a simple model, and the effect is stronger in fainter magnitude.

We can therefore think that ‘‘If one tries to match the distribution of faint stars, which should have low metallicity, with that of higher metallicity stars (such as BPGS and GS83) by tuning the ZP, incorrect shifts might be introduced.’’ The second step of the SDF and SXDS calibration may have suffered this effect.

In figure 17 we plot color-color diagrams in Suprime-Cam color for SDF and SXDS-C. The stars matched with the SDSS catalog are used, and magnitude cut based on SDSS magnitude is applied; $20.5 < g < 21.5$ for (X-V) vs (V-Y), $20 < r < 21$ for (X-R) vs (R-Y), and $19.5 < i < 20.5$ for (X-i) vs (i-Y), where $X=(B,V,R)$ and $Y=(R,i,z)$. The magnitude range is the same as that for the calibration in the previous section. The filled black circles are the values in the catalog. The estimated ZP offset in table 5 is shown as a blue arrow. The filled circles represent the model colors; $[\text{Fe}/\text{H}]=0$ model in green and $[\text{Fe}/\text{H}]=-2.5a$ model in red, as in figure 14.

SDF B-band offset is understood by this metallicity effect. The original calibration follows the $[\text{Fe}/\text{H}]=0$ models and the arrow shows that it should rather follow $[\text{Fe}/\text{H}]=-2.5a$ models. Since Furusawa et al. (2008) did not shift the B-band of SXDS, the distribution is free from the metallicity effect, and it would be the reason the B-band ZP

offset of SXDS from SDSS is small (≤ 0.02 mag).

4.2.2. Previous Catalog of SXDS Region

The calibration of SXDS depends on the calibration by Ouchi et al. (2004). We refer to the catalog by Ouchi et al. (2004) as the GT-SXDF-catalog hereafter. The B,V,R and i-band data of GT-SXDF-catalog were obtained in November and December 2000. Additional R-band data and z-band data were obtained in September 2001. We investigated the GT-SXDF-catalog which was used for the calibration of SXDS DR1 catalog, whether they also show an offset from SDSS.

In November and December 2000, the CCD configuration of Suprime-Cam was heterogeneous; four SITE CCDs, three MIT/LL engineering CCDs with a brickwall pattern (we call them MIT0), and two MIT/LL scientific-grade CCDs without a brickwall pattern (MIT1). The three different types of CCDs have different QE functions. In April 2001, the MIT0 and SITE chips were replaced with MIT1 CCDs. The SDF and SXDS DR1 data re-calibrated in this study were obtained with the MIT1 CCDs.

In figure 18, the SDSS color versus (SDSS)-(Suprime-Cam) magnitude are plotted using the GT-SXDF-catalog. We simply classified the stars in the GT-SXDF-catalog to the nearest CCD group. Therefore, misclassifications and/or hybrids may contaminate. In Ouchi et al. (2004), they adopted the 2 arcsec aperture magnitude with 0.2 mag aperture correction, but we adopt MAG_AUTO as in the plot as Furusawa et al. (2008). For figure 18, we adopted a slightly different magnitude selection from figure 9 as $20.5 < g < 21.5$ for B and V, $20 < r < 21$ for R, $20.5 < i < 19$ for i, and $19.5 < z < 18.5$ for z. As R-band is a coadd of data taken with old CCDs and MIT1 CCDs, and MIT1 model is overplotted, though the difference is indistinguishable.

The GT-SXDF-catalog was calibrated as the AB magnitude with the SITE response as done in Ouchi (2001), which is slightly different from the MIT1 response adopted in SXDS. It might have contributed partly to the offset of ZP of SXDS in B-band. In the B-band MIT0 plot, the color slope is different between the model and the catalog, suggesting that the CCD response used in the calculation was wrong at shorter wavelength. It is reported that the linearity of MIT/LL CCDs was not so good from October 2000 to December 2000¹⁶¹⁷. The effect of the correction on the ZP is unclear, though.

In i and z-band, the offset in the ZP from the estimation is already seen in the GT-SXDF-catalog. It should be noted that the CCDs used in z-band are the same as those for the SXDS catalog, and the offset is not from the difference of CCD responses.

Unfortunately, the details of the first step of the standard star calibration for the GT-SXDF-catalog were lost because of a hardware failure (Ouchi, M., 2012, private communication). We cannot unveil the history further.

¹⁶ <http://smoka.nao.ac.jp/about/subaru.jsp>

¹⁷ <http://anela.mtk.nao.ac.jp/suprime/report/linearity.pdf>

4.2.3. Standard Star for SXDS i-band

For i-band in SXDS¹⁸, synthetic magnitude of SA95-42 calculated from spectrophotometric data by Oke (1990) was used (Ouchi 2001; Ouchi et al. 2004; Furusawa et al. 2008), and the synthetic magnitude of 16.23 was adopted. We noticed that Oke’s spectrum is different from that of SDSS as shown in figure 19. The SDSS i-band magnitude calculated from SDSS spectrum (16.11) is 0.12 mag brighter. In SDSS DR8 photometric data, meanwhile, the magnitude of SA95-42 is 16.16 after the AB-SDSS correction of 0.028 by Kcorrect v4. The SDSS i-band AB magnitude of SA95-42 has thus not converged. It might be an origin of the ~ 0.1 mag dimming of SXDS catalog and GT-SXDF-catalog from SDSS. And since both i-band and z-band had offsets in the ZP in the SXDS catalog, the offsets in both bands would not have been fully corrected in the comparison with the GS83 distribution.

4.2.4. The i-band and z-band Magnitude of Standard Stars for SDF

The spectrophotometric standard stars used in SDF for i and z-band are HZ21, HZ44, GD153, P177D, and P330E (Kashikawa et al. 2004). They are originally from Oke (1990); Bohlin et al. (2001); Bohlin (2003), and are available at STSci sites^{19,20}. The stars do not have SDSS spectra, but have psfMag in SDSS DR8. The difference of the i and z-band PSF magnitudes of SDSS DR8 and the synthetic magnitudes using Doi et al. (2010) transmission and the SED are shown in table 6. The offset given by Kcorrect v4 is applied to SDSS magnitude in the table. The error shows the SDSS catalog error (psfMag_err). The version of the SED used for the analysis of SDF and adopted magnitude were lost and we cannot investigate the historical detail. However, the difference is mostly too small (<0.04 mag, except for z of HZ44 and i of GD153) to explain the 0.1 mag offset we found. Moreover, the sign of the GD153 offset in i-band (+0.14 mag) is opposite to the ZP offset we found. In our analysis, SDF stars are fainter than SDSS, while the synthetic magnitude of GD153 is brighter than SDSS. Therefore, the i-band and z-band magnitude difference of SDF may not be explained only by some error of spectrophotometric standards.

5. Summary

Using SDSS, we found an offset of the ZP of SDF and SXDS. We present a robust color conversion from SDSS to the Suprime-Cam system. The color conversion is robust against the difference in metallicity, Galactic extinction, atmospheric extinction, and recession velocity of the stars. And the offset of ZP is then calculated against SDSS.

If we applied the correction of the offset we obtained, the difference in the color distribution of faint ($R \sim 24$)

objects in SDF and SXDS disappears. The result supports that the relative color difference between SDF and SXDS is corrected well by our result. And since the relative color offset of SDF and SXDS of bright stars ($R \sim 20$) and at the faint object are consistent, it should be explained by a simple offset of the ZP.

The B-band offset of SDF would be explained by the difference of the color of stars in the data and the adopted references, due to the different metallicity. The i and z-band of SXDS inherited the offset in the previous catalog. The magnitude of i-band standard star SXDS adopted (SA95-42) has a offset ($\gtrsim 0.07$) from SDSS, which may be the origin of the SXDS i-band offset. The origin of the offset of SDF i-band and SDF/SXDS z-band are yet to be understood.

We thank the anonymous referee for valuable comments and suggestions. We appreciate Masayuki Tanaka, Masami Ouchi, Nobunari Kashikawa, and Kazuhiro Shimasaku for their suggestive comments, indications, and information. The SDF catalog and SXDS catalog are obtained from Astronomy Data Center (ADC) at the National Astronomical Observatory of Japan. This work has made use of the SDSS database and the computer systems at ADC.

References

- Abazajian, K.N. et al. 2009, ApJS, 182, 543
 Adelman-McCarthy, J.K. et al. 2008, ApJS, 175, 297
 Aihara, H. et al. 2011, ApJS, 193, 29
 Blanton, M.R., Roweis, S. 2007, AJ, 133, 734
 Bohlin, R.C., Dickinson, M.E. and Calzetti, D. 2001, AJ, 122, 2118
 Bohlin, R.C., in The 2002 HST Calibration Workshop, ed. S. Arribas, A. Koekemoer, & B. Whitmore (Baltimore: STSci), 115
 Bohlin, R.C. 2010, AJ, 139, 1515
 Cardelli, J.A., Clayton, G.C. & Mathis, J.S. 1989, ApJ, 345, 245
 Castelli, F., Kurucz, R.L. 2004, arXiv astro-ph/0405087
 Ciddor, P.E. 1996, Applied Optics, 35, 1566
 Demarque, P., Woo, J.-H., Kim, Y.-C., Yi, S.K. 2004, ApJS, 155, 667
 Doi, M. et al. 2010, AJ, 139, 1628
 Fukugita, M., Shimasaku, K., Ichikawa, T, PASP, 107, 945
 Fukugita, M., Yasuda, N., Doi, M., Gunn, J.E., York, D.G. 2011, AJ, 141, 47
 Furusawa, H. et al. 2008, ApJS, 176, 1
 Furusawa, J. et al. 2011, ApJ, 727, 111
 Green, E.M., Demarque, P., King, C.R. 1987, The revised Yale isochrones and luminosity functions (New Haven: Yale Observatory)
 Gunn, J.E., Stryker, L.L. 1983, ApJS, 52, 121
 Hayashi, M. et al. 2007, ApJ, 660, 72
 Jurić et al. 2008, ApJ, 673, 864
 Kashikawa, N. et al. 2004, PASJ, 56, 1011
 Kashikawa, N. et al. 2006, ApJ, 637, 631
 Landolt, A.U. 2009, AJ, 137, 4186
 Le Borgne, J.-F., Bruzual, G., Pelló, R., Lançon, A., Rocca-Volmerange, B., Sanahuja, B., Schaerer, D., Soubiran, C., Vílchez-Gómez, R. 2003, A&A, 402, 433

¹⁸ For z-band calibration of SXDS, Ouchi et al. (2004) and Furusawa et al. (2008) wrote that SA95-42 is used. We however found that SA95-42 was not observed in z-band when the field was observed. We guess that GD71 should actually be used in Ouchi et al. (2004).

¹⁹ <http://www.stsci.edu/hst/observatory/cdbs/calspec.html>

²⁰ <ftp://ftp.stsci.edu/cdbs/oldcalspec/>

- Lenz, D.D., Newberg, J., Rosner, R., Richards, G.T.,
Stoughton, C. 1998, ApJS, 119, 121
- Lupton, R.H., Gunn, J.E., Szalay, A.S. 1999, AJ, 118, 1406
- Miyazaki, S., et al. 2002, PASJ, 54, 833
- Morton, D.C. 1991, ApJS, 77, 119
- O'Donnell, J.E. 1994, ApJ, 422, 158
- Oke, J.B., Gunn, J.E. 1983, ApJ, 266, 713
- Oke, J.B., 1990, AJ, 99, 1621
- Ouchi, M. 2001, master thesis for the University of Tokyo
- Ouchi, M. et al. 2001, ApJL, 558, L83
- Ouchi, M. et al. 2004, ApJ, 611, 660
- Ouchi, M. et al. 2005, ApJL, 635, L117
- Padmanabhan, N. et al., ApJ, 674, 1217
- Peng, X., Cu, C., Wu, Z. 2012, MNRAS, 422, 2756
- Pickles, A. 1998, PASP, 110, 863
- Pogson, N. 1856, MNRAS, 17, 12
- Schlafly, E.F., Finkbeiner, D.P., 2011, ApJ, 737, 103
- Stevenson, C.C. 1994, MNRAS, 267, 904
- Takata, T. et al. 2000, Proc. SPIE, 4010, 181
- Toshikawa, J. et al. 2012, ApJ, 750, 137
- Valdes, F., Gupta, R, Rose, J.A.; S., H.P.; Bell, D.J. 2004,
ApJS, 152, 251
- Yagi, M. et al. 2010, AJ, 140, 1814
- Yamanoi, H. et al. 2012, AJ, 144, 40
- Yi, S., Demarque, P., Kim, Y.-C., Lee, Y.-W., Ree, C.H.,
Lejeune, T., Barnes, S. 2001, ApJS, 136, 417

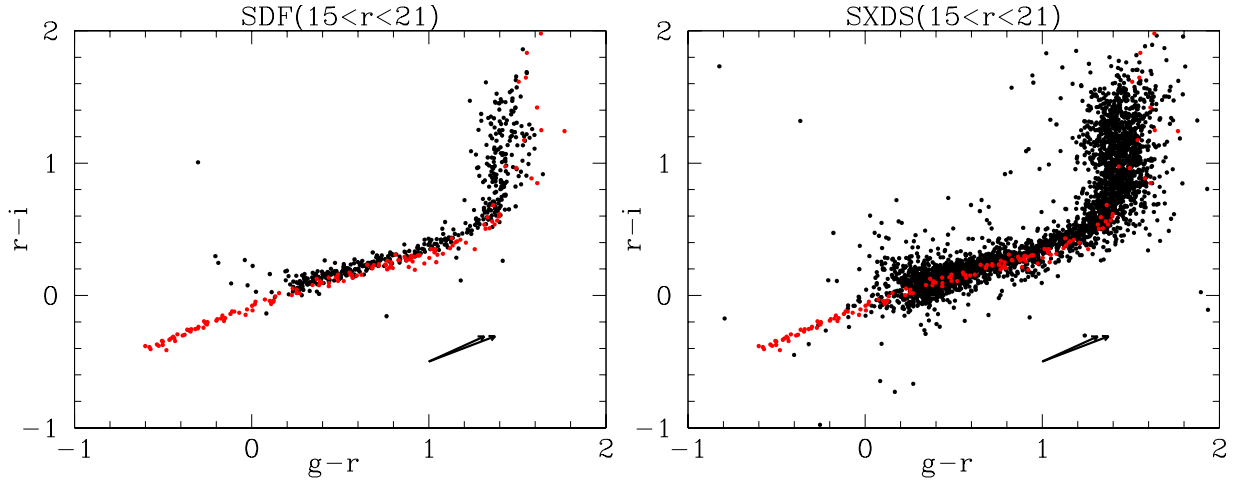


Fig. 1. Color-color diagram of SDSS DR8 stars of $15 < r < 21$ in SDF(left) and SXDS(right) field. The color of SDSS stars is calculated from psfMag. The offset of $m_{AB} - m_{SDSS}$ given by Kcorrect (Blanton & Roweis 2007) v4 is applied. The filled red circles represent synthetic colors of GS83 stars calculated with the transmission by Doi et al. (2010). The arrows indicate the direction of $A_V=1$ reddening of Galactic extinction for O and M stars in GS83.

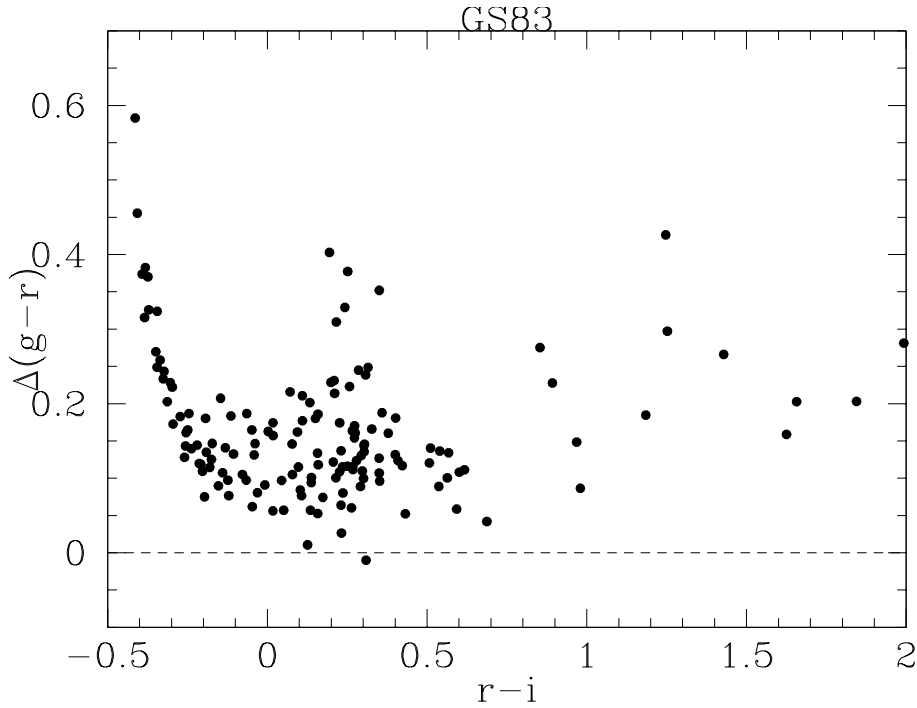


Fig. 2. The difference of $(g-r)$ color of GS83 stars from the analytic fit of SDSS stars by Jurić et al. (2008) as a function of $(r-i)$. $\Delta(g-r)=0$ is shown as a broken line for comparison.

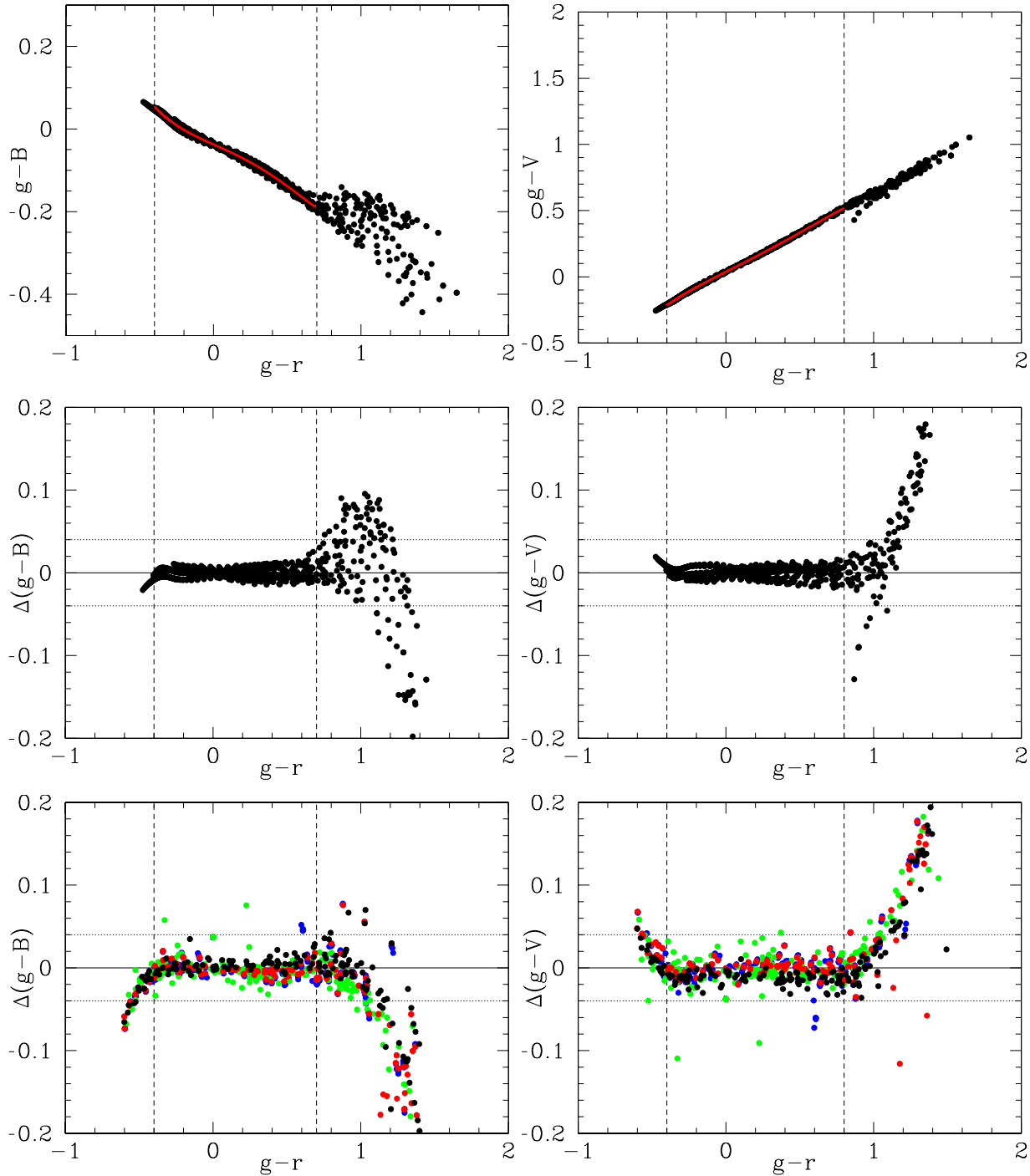


Fig. 3. (top) Fitting of polynomial to the synthetic color of SDSS minus Suprime-Cam color as a function of SDSS color. The model adopts atmospheric extinction at airmass=1, and no Galactic extinction. The red line represents the fit function and the dots are the model colors. (middle) Residual of model color from the best-fit function. Vertical lines represent the fitting color range. Horizontal lines are 0 and ± 0.04 mag for reference. The filled black circles are ATLAS9 models. (bottom) Residual of SDSS minus Suprime-Cam color of various SEDs; CFLIB, STELIB, HILIB, and BPGS in blue, green, red and black, respectively. The vertical and the horizontal lines are the same as the middle panel.

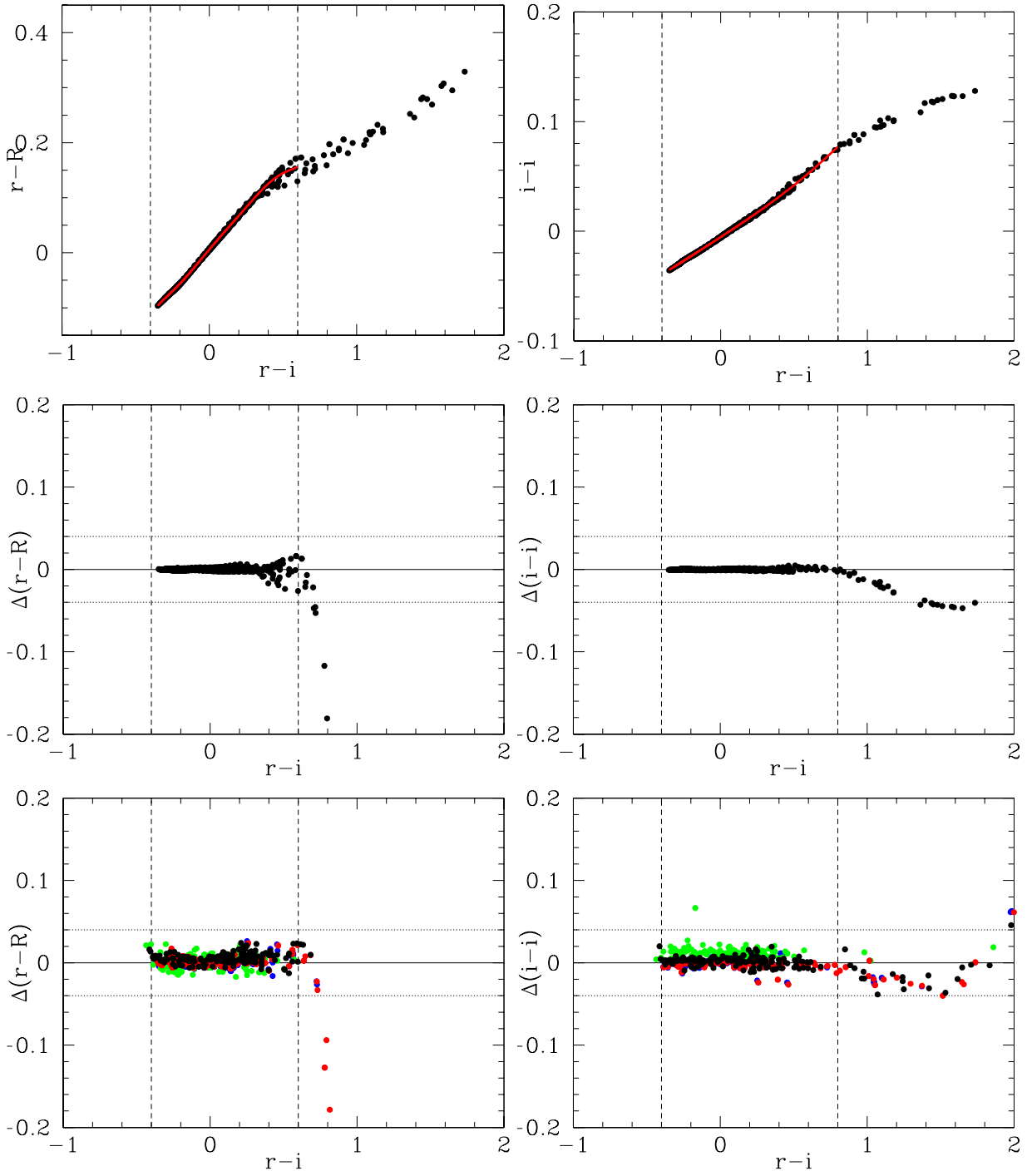


Fig. 3. Continued...

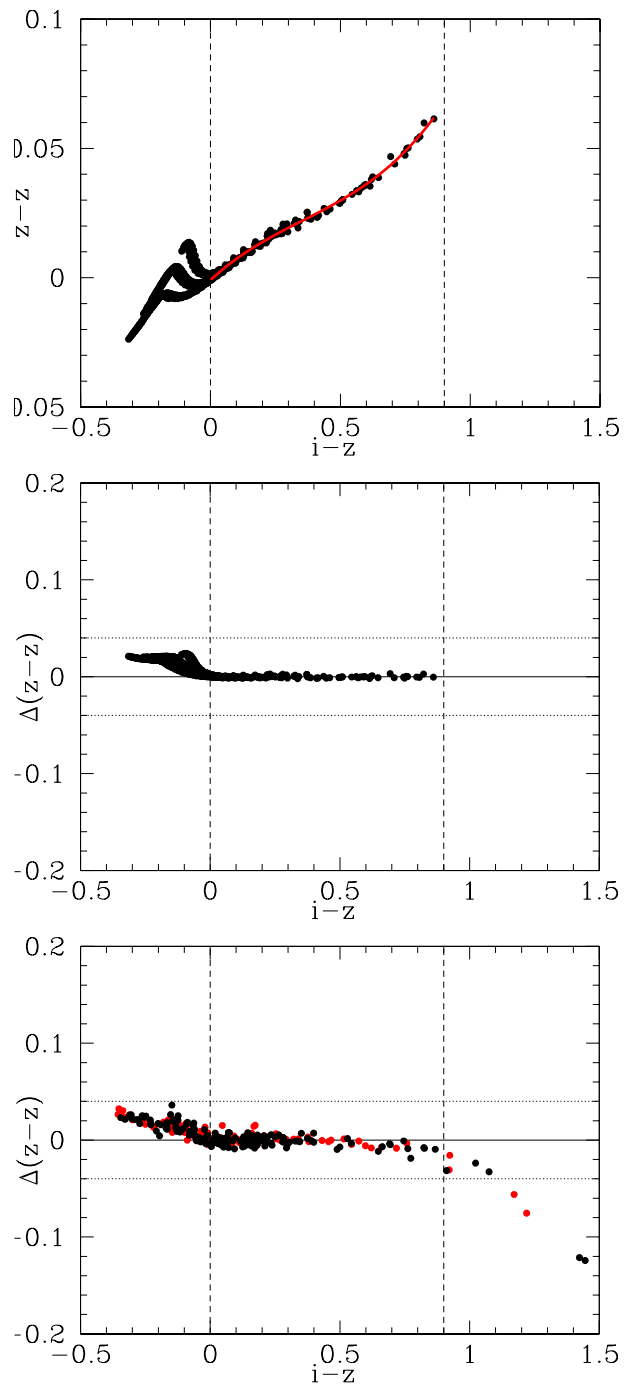


Fig. 3. Continued...

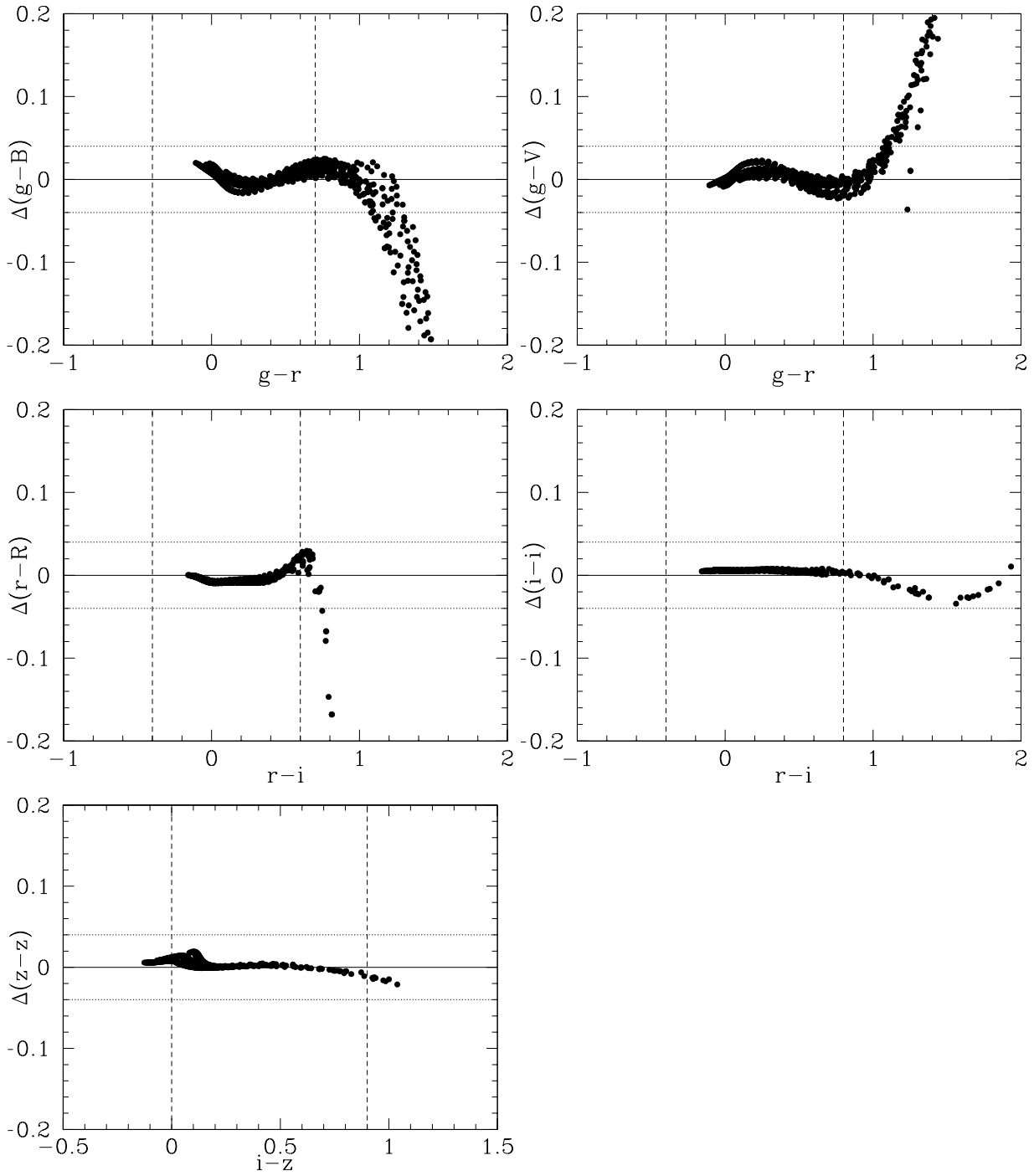


Fig. 4. Same as the middle panel of figure 3. but an extreme $A_v=1$ mag extinction is applied to the model.

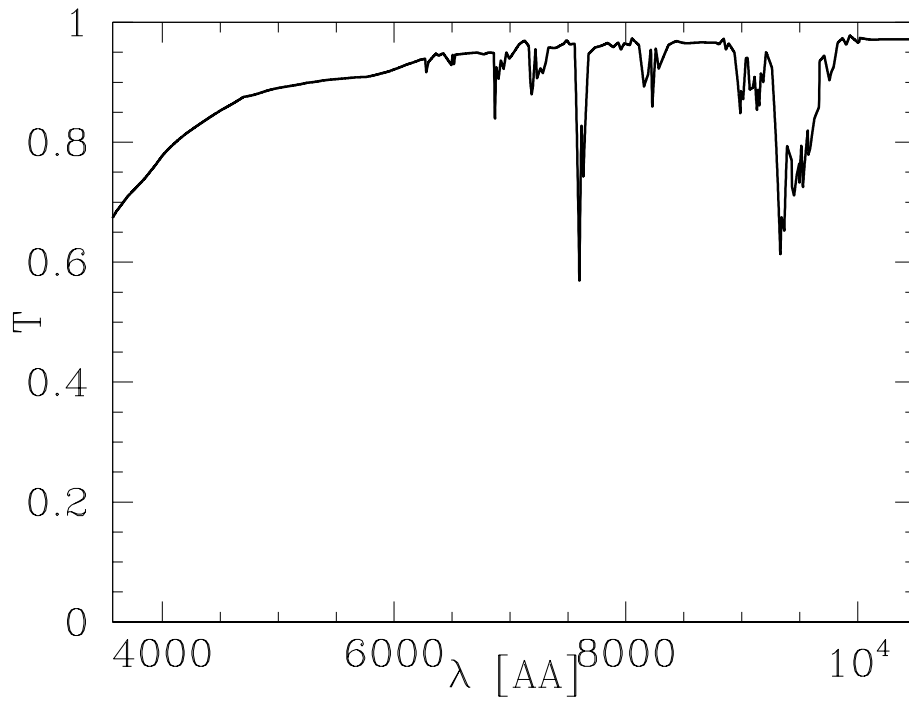


Fig. 5. The airmass=1 sky extinction model at Subaru used in this study.

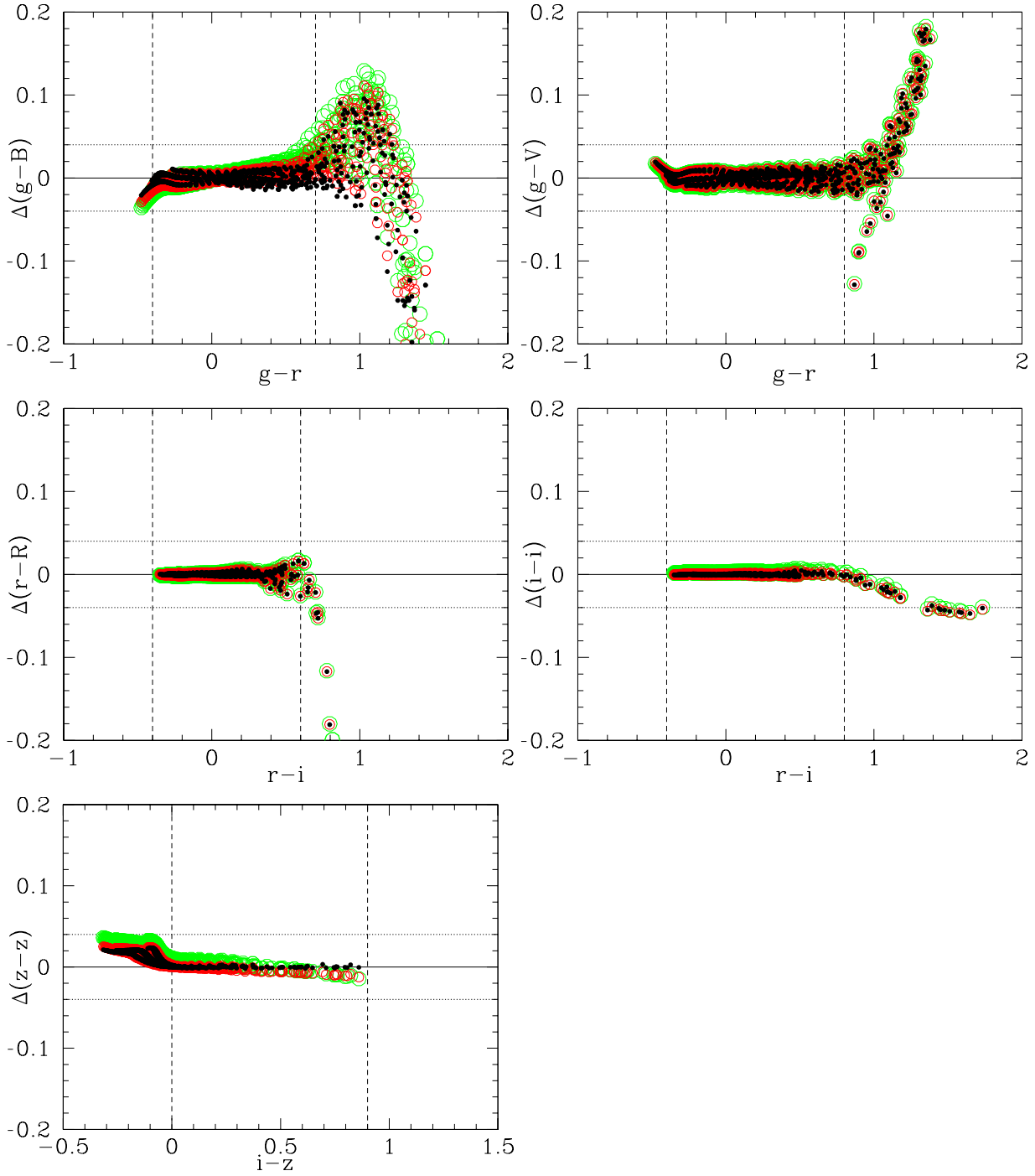


Fig. 6. Residual of model color from the best-fit function. Vertical lines represent the fitting color range, and horizontal lines are 0 and ± 0.04 mag for reference. The different airmass models are plotted; airmass=1(black filled circles), airmass=2(red open circles) and airmass=3(green open circles). A linear term of airmass k_1 (airmass-1) is corrected for the airmass=2 and 3 models.

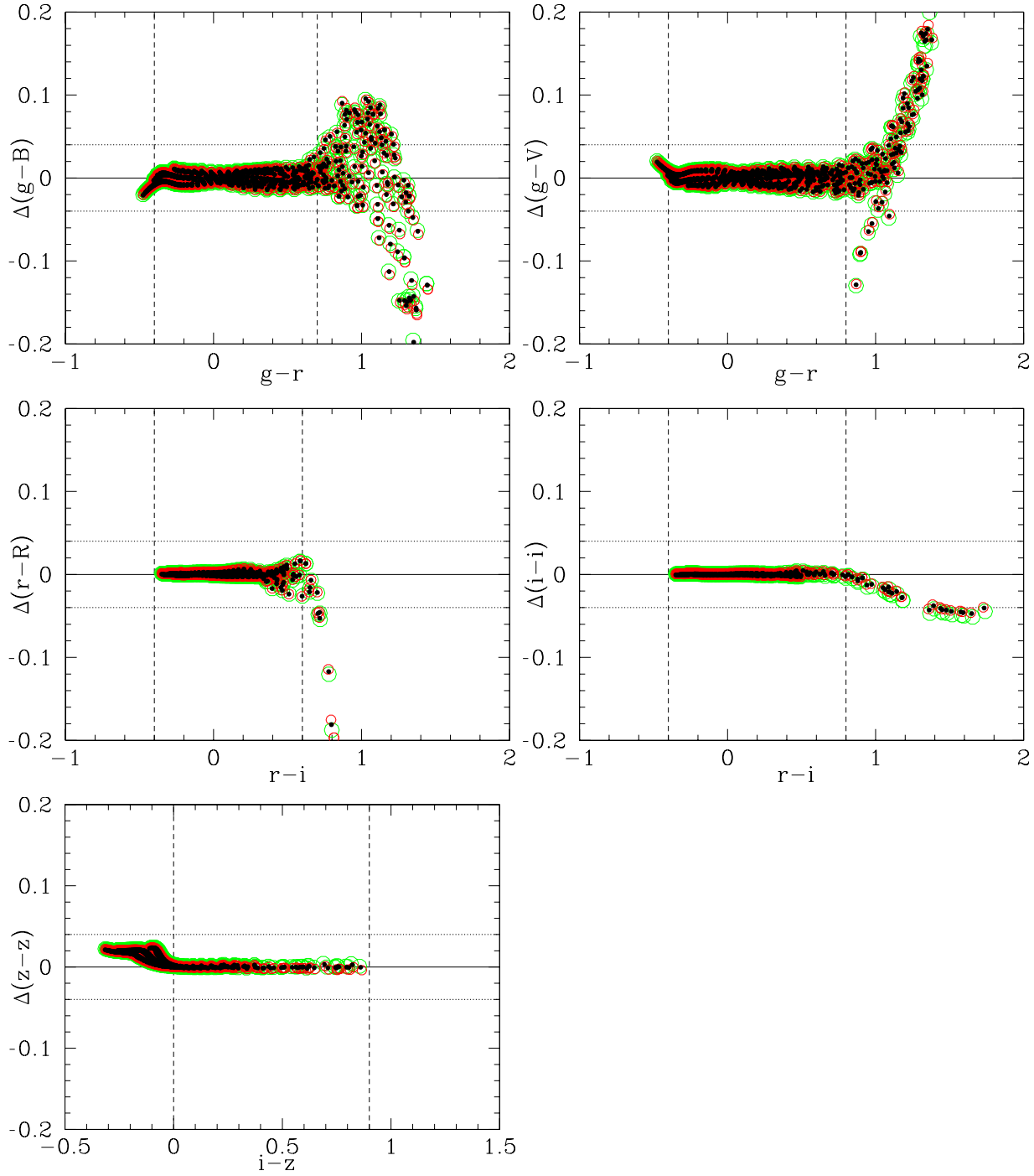


Fig. 7. Same as figure 6 but airmass=1 with different recession velocities; $v_r=0 \text{ km s}^{-1}$ model in black filled circles, $v_r=+300 \text{ km s}^{-1}$ model in red open circles, and $v_r=-300 \text{ km s}^{-1}$ model in green open circles.

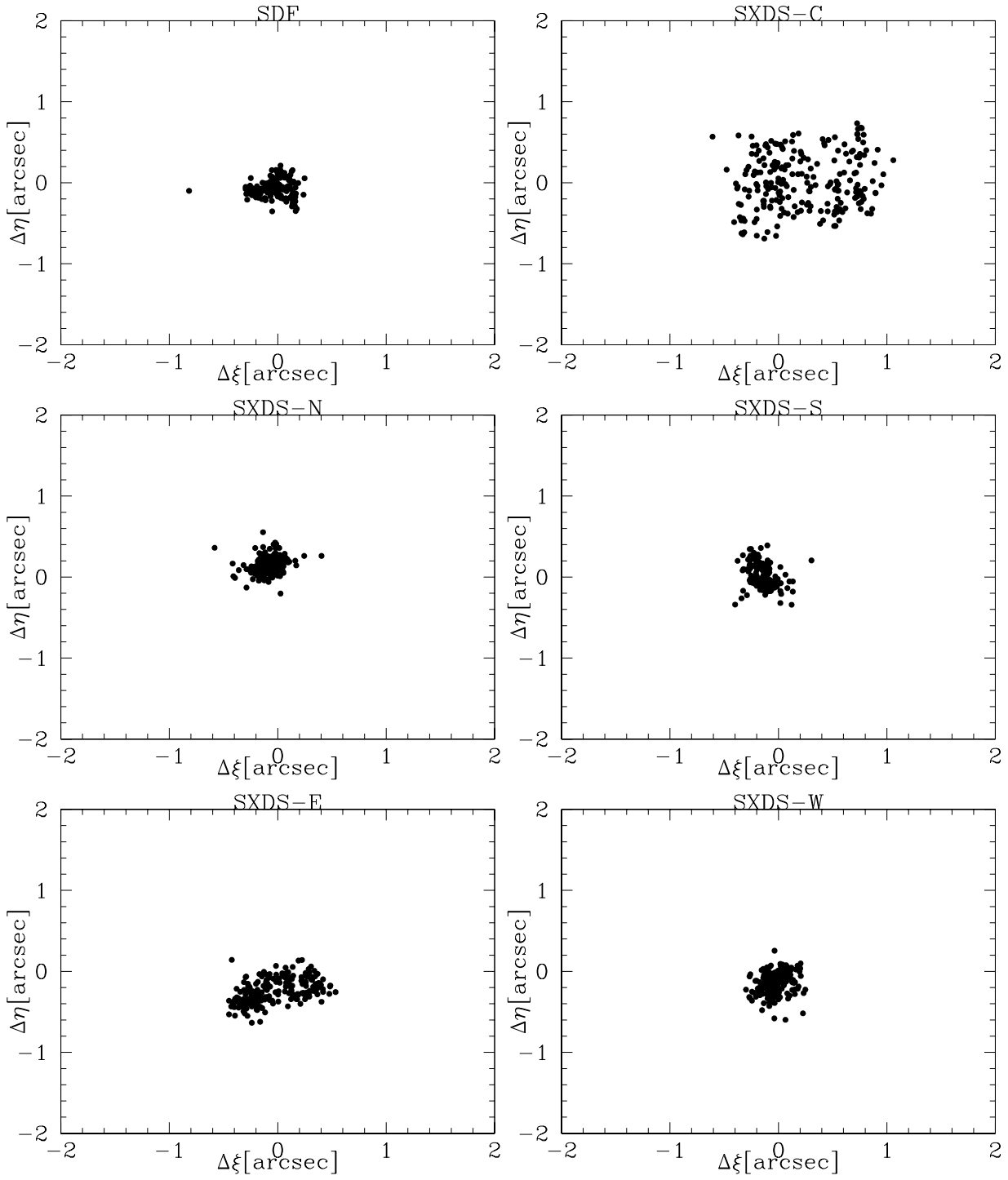


Fig. 8. The difference of the position of matched stars in $20 < r < 21$ magnitude range. $\Delta\xi = \alpha \cos(\delta)(\text{SDSS}) - \alpha \cos(\delta)(\text{Suprime - Cam})$, and $\Delta\eta = \delta(\text{SDSS}) - \delta(\text{Suprime - Cam})$.

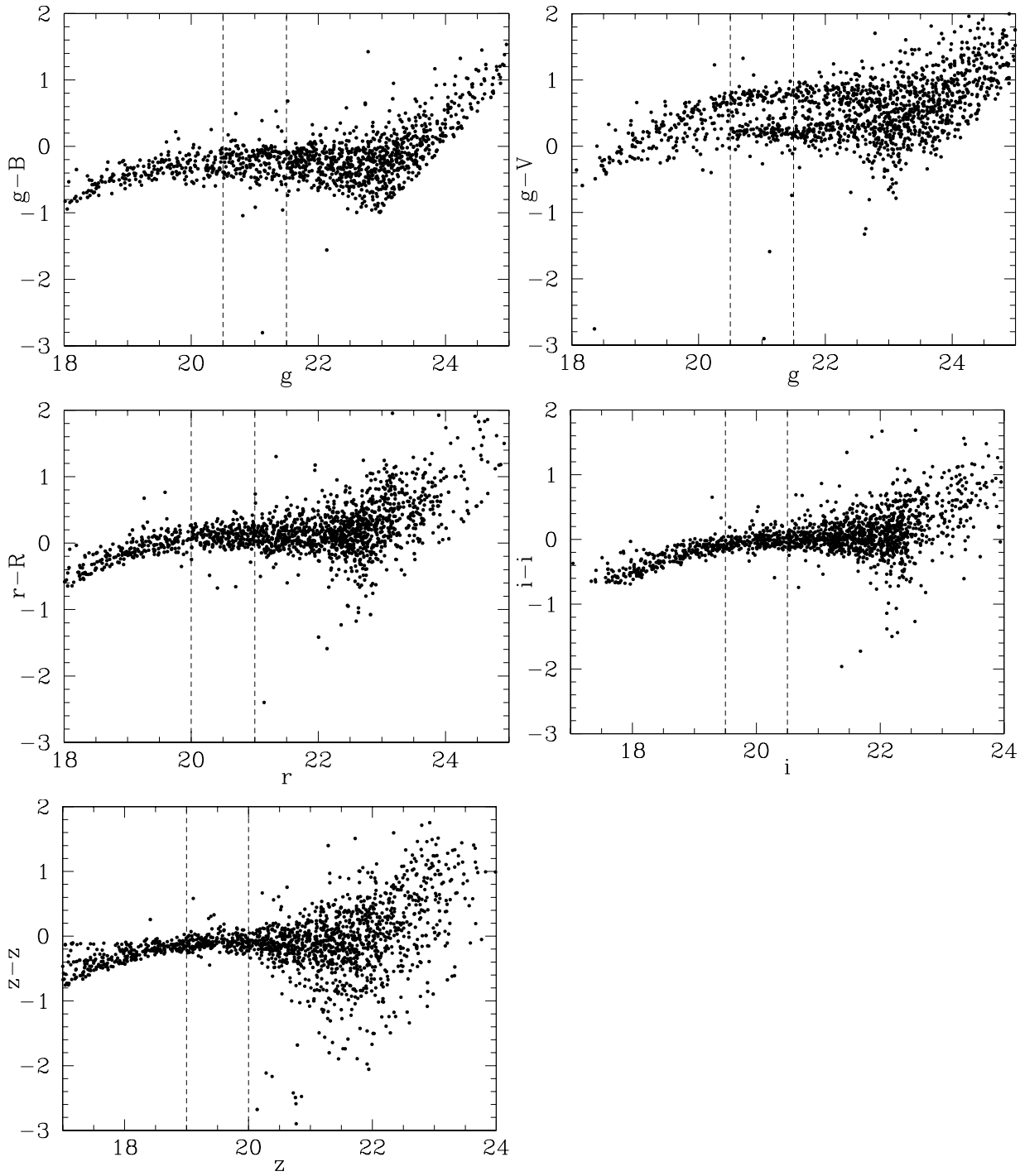


Fig. 9. Color magnitude diagram of (SDSS)-(Suprime-Cam) matched stars in SDF field. The cutoff of the left bottom side is due to the Suprime-Cam magnitude cut of $\text{mag} < 24$. The vertical lines show the adopted magnitude range for the calibration.

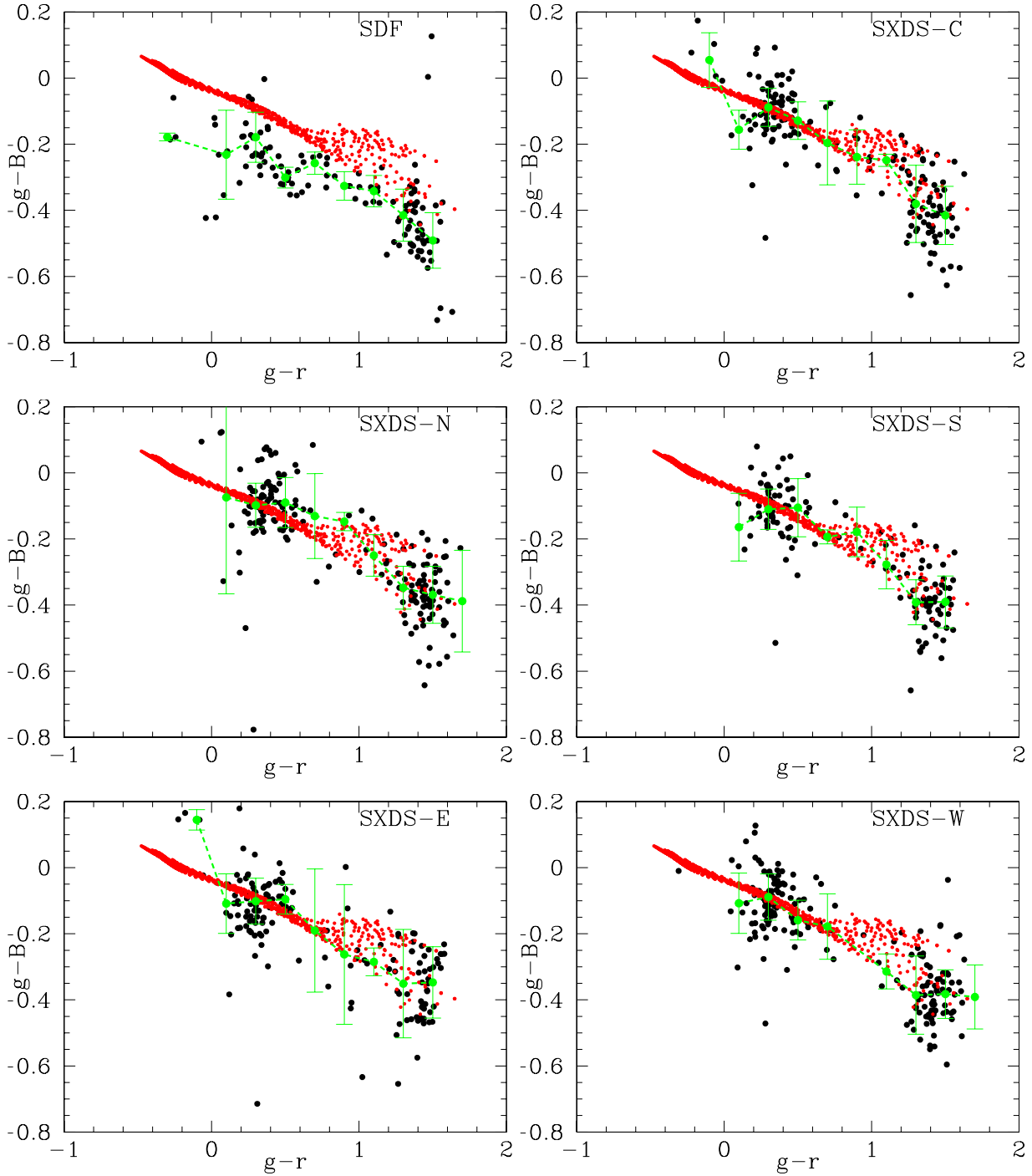


Fig. 10. SDSS color versus the (SDSS)-(Suprime-Cam) color. Top-left panel is SDF and other panels are SXDS. The filled circles represent matched stars. The magnitude ranges are $20.5 < g < 21.5$ for B and V, $20 < r < 21$ for R, $19.5 < i < 20.5$ for i, and $19 < z < 20$ for z. The filled red circles are ATLAS9 model colors, which are shown as filled black circles in left panels of figure 3. The filled green circles with errorbar show the median of the (SDSS)-(Suprime-Cam) color in 0.2 mag bin of SDSS color. The errorbar represents rms estimated from MAD of the bin.

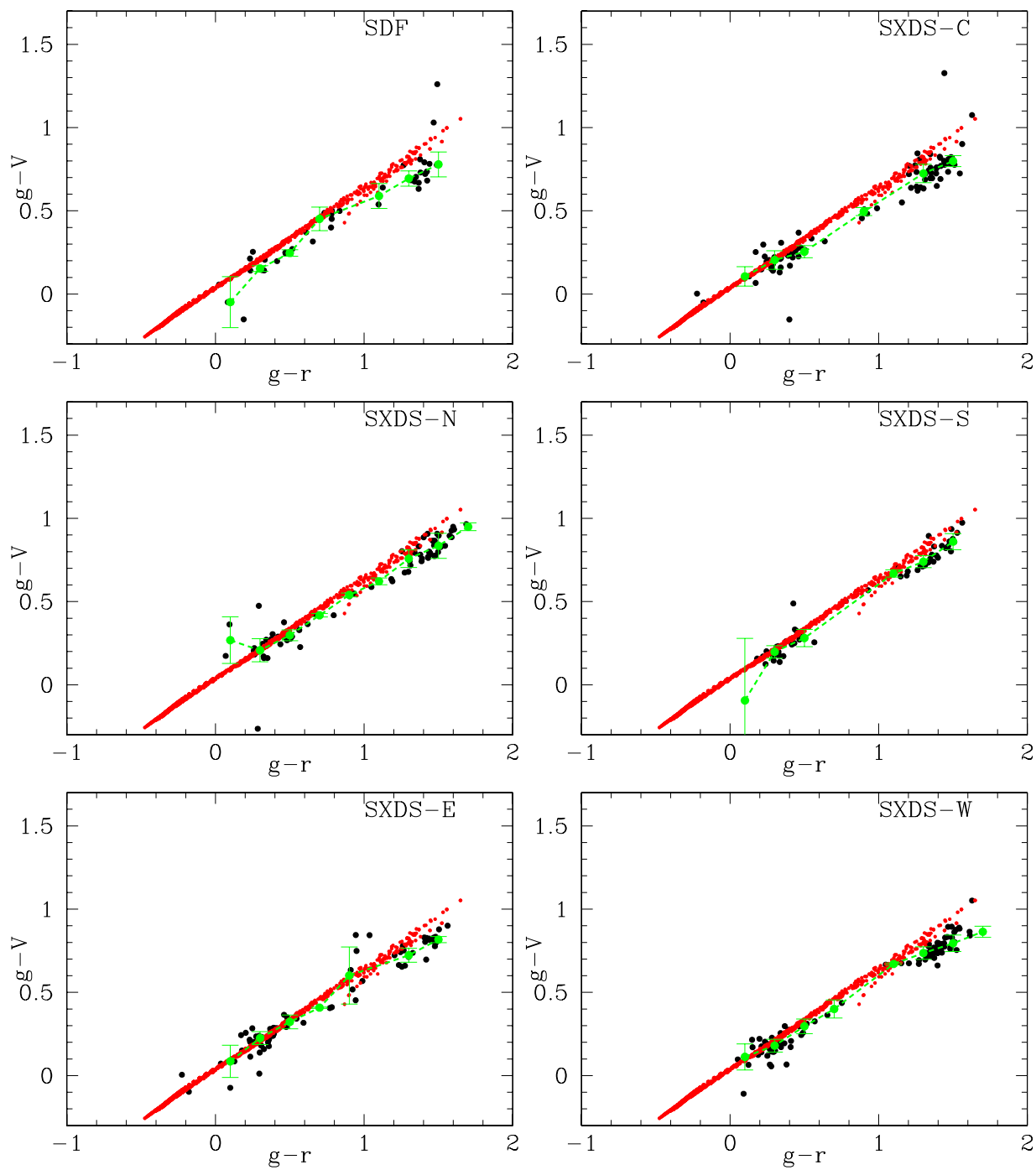


Fig. 10. Continued...

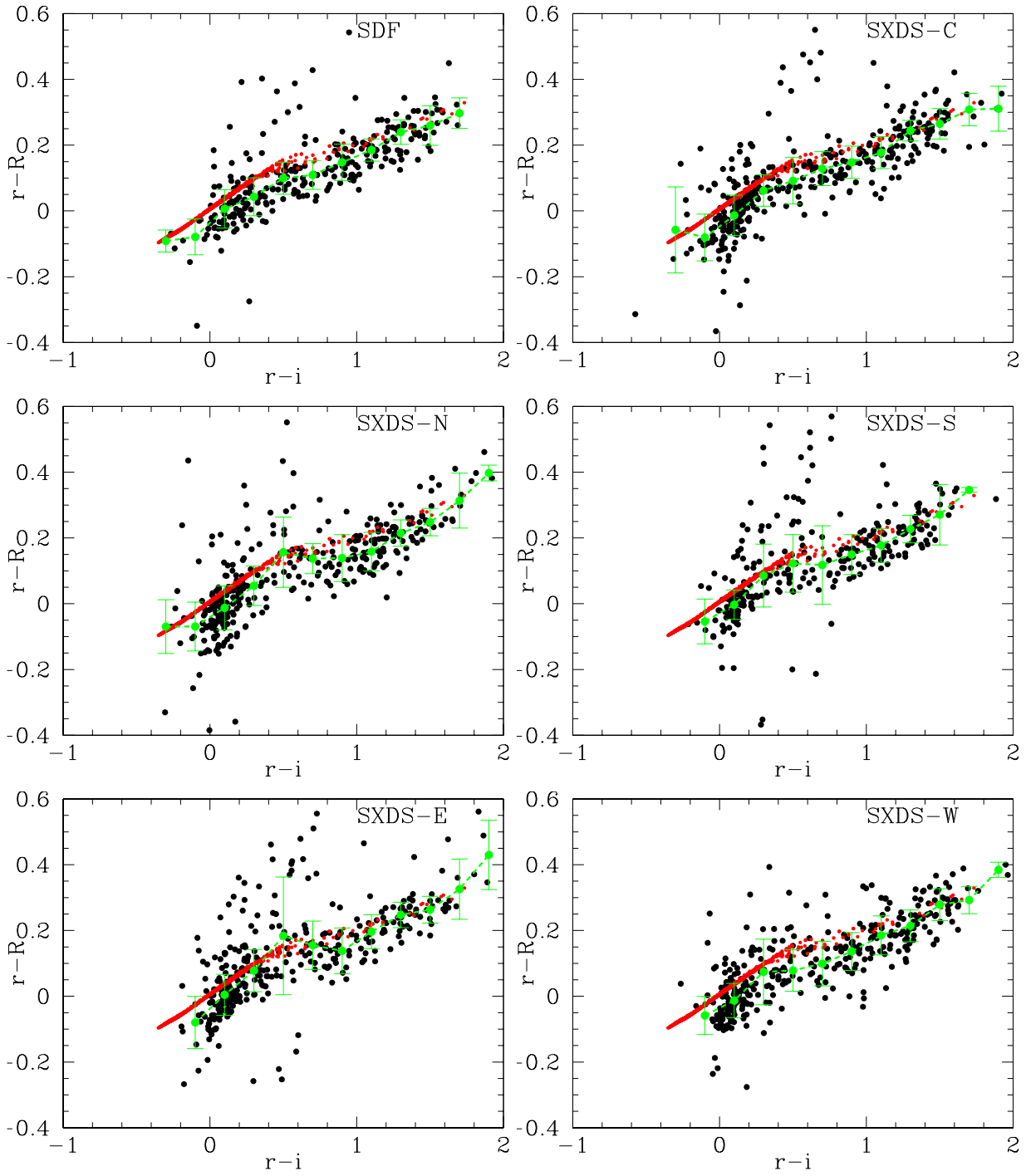


Fig. 10. Continued...

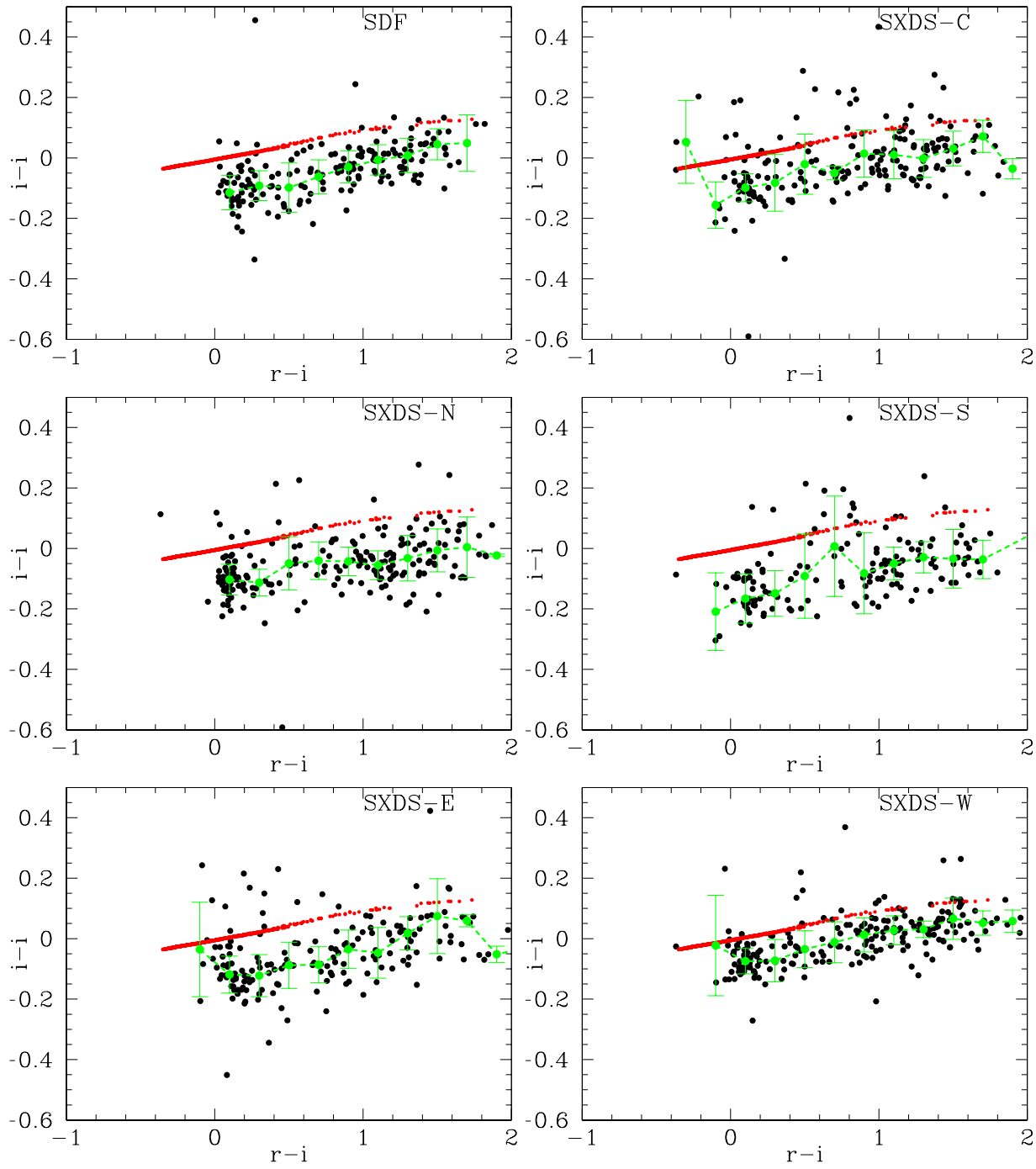


Fig. 10. Continued...

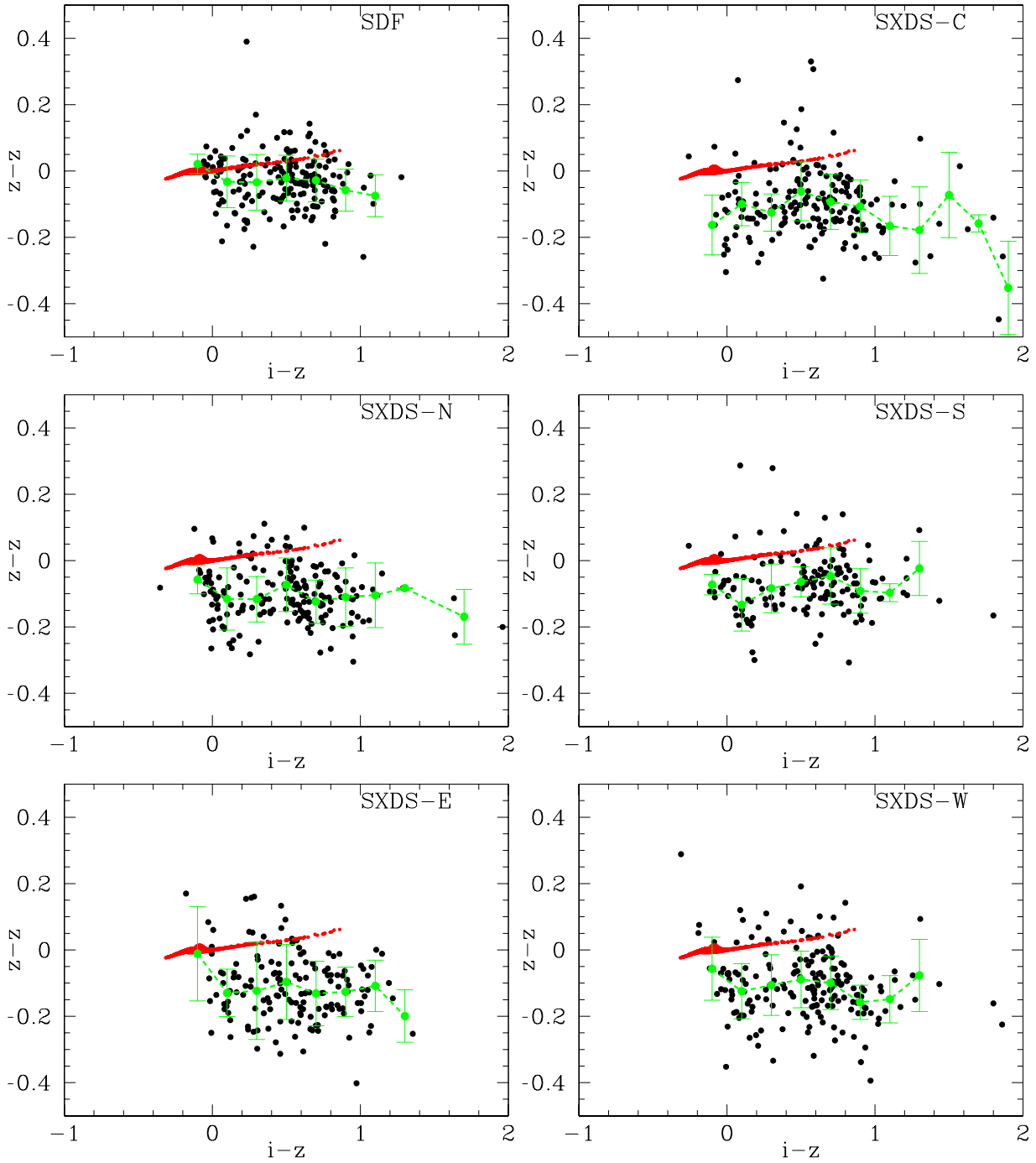


Fig. 10. Continued...

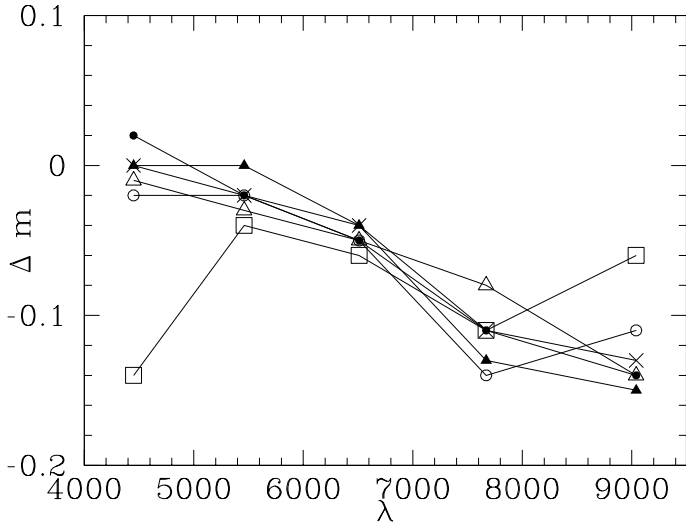


Fig. 11. The ZP difference between the catalog and the estimated value from SDSS as a function of the wavelength of filters. The symbols represent field as open squares (SDF), the crosses (SXDS-C), the filled circles (SXDS-N), the open circles (SXDS-S), the filled triangles (SXDS-E), and the open triangles (SXDS-W). The data of the same field are connected by a line.

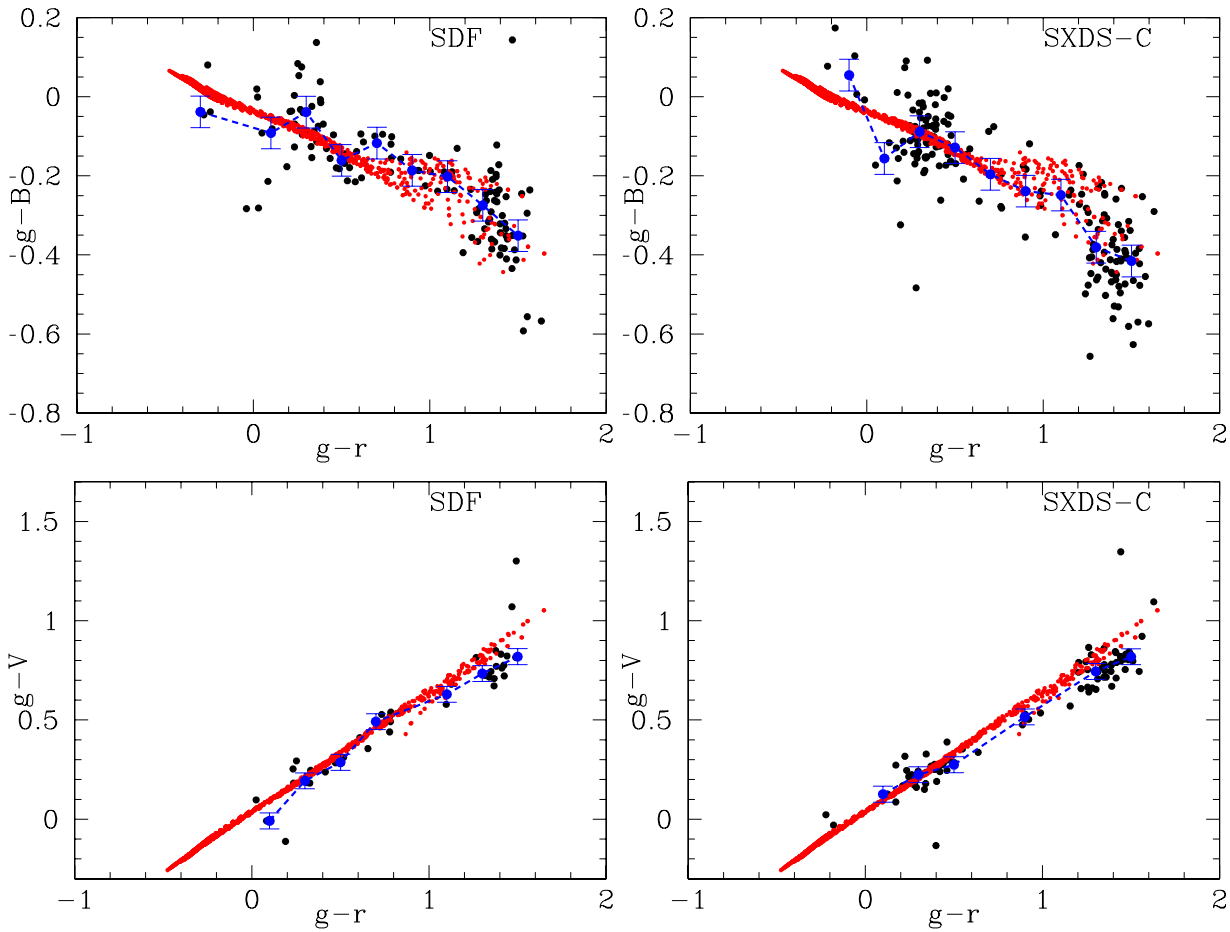


Fig. 12. Same as figure 10, but after the ZP offset correction, and errorbars are fixed as 0.04 mag. Only SDF and SXDS-C are shown.

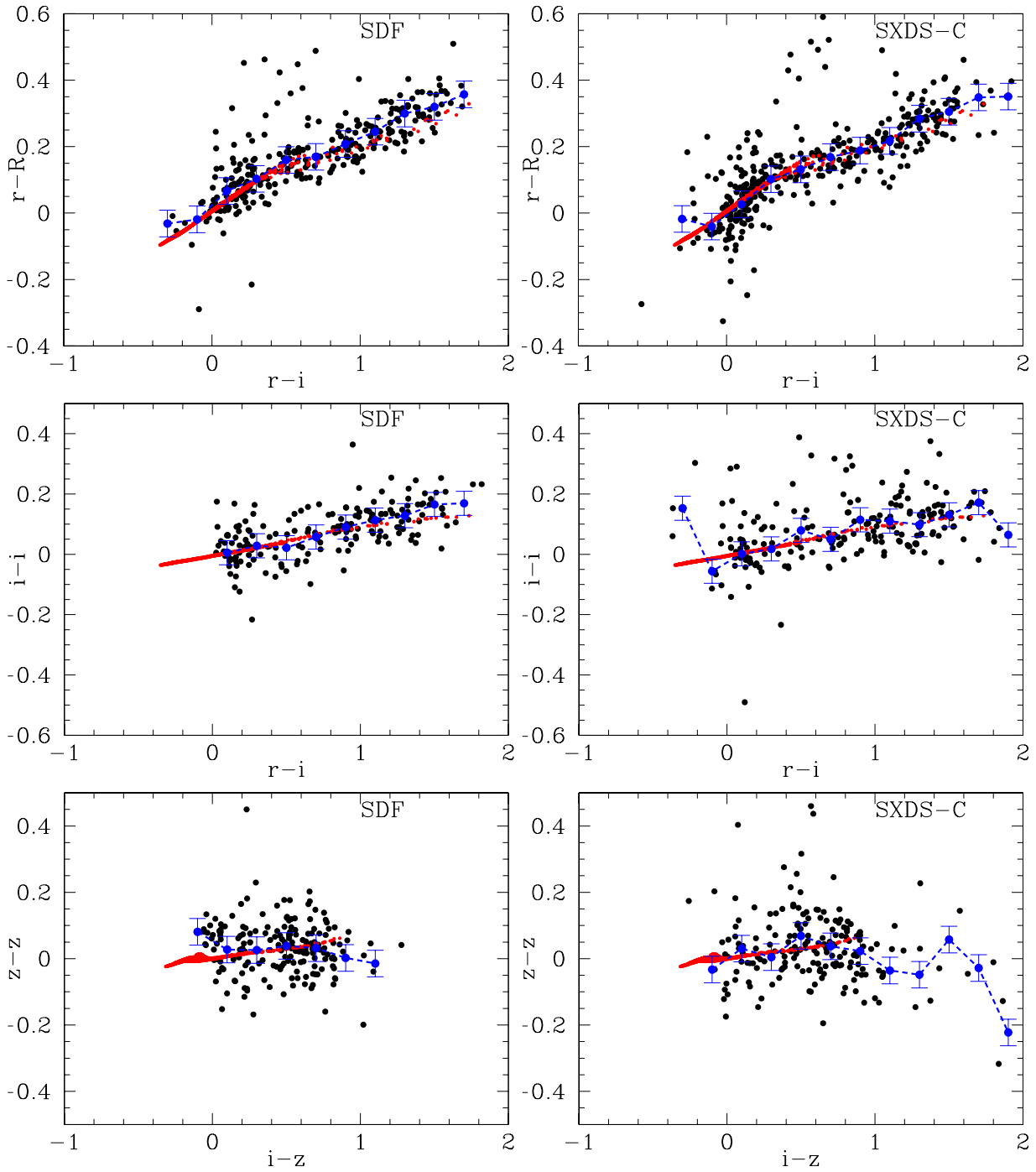


Fig. 12. Continued...

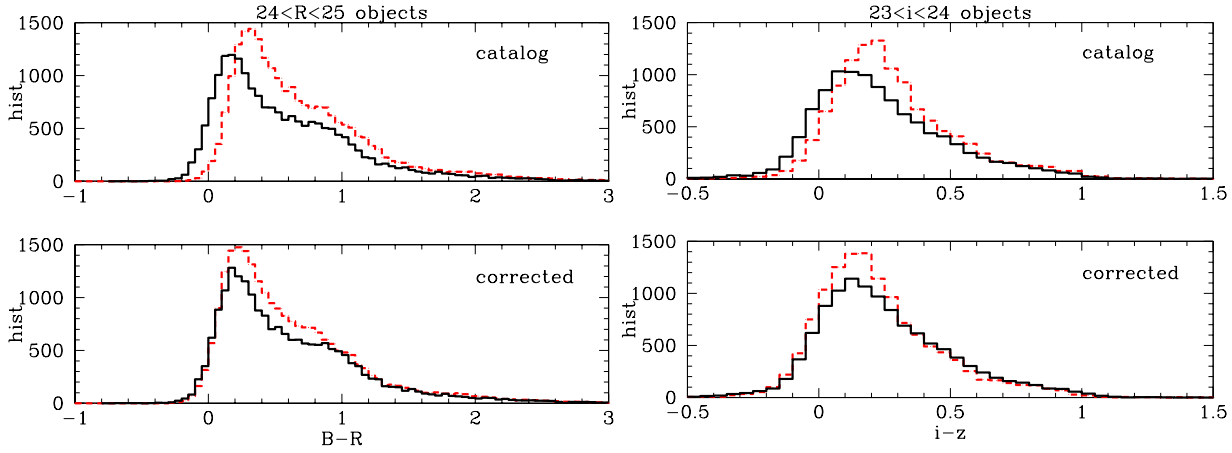


Fig. 13. (left) (B-R) color histogram of $24 < R < 25$ objects in SDF (dashed red) and SXDS (solid black). The top panel uses the catalog value, and the bottom panel uses the value with the correction in table 5. Galactic extinction is corrected. (right) Same as the left panel but of (i-z) color of $23 < i < 24$ objects.

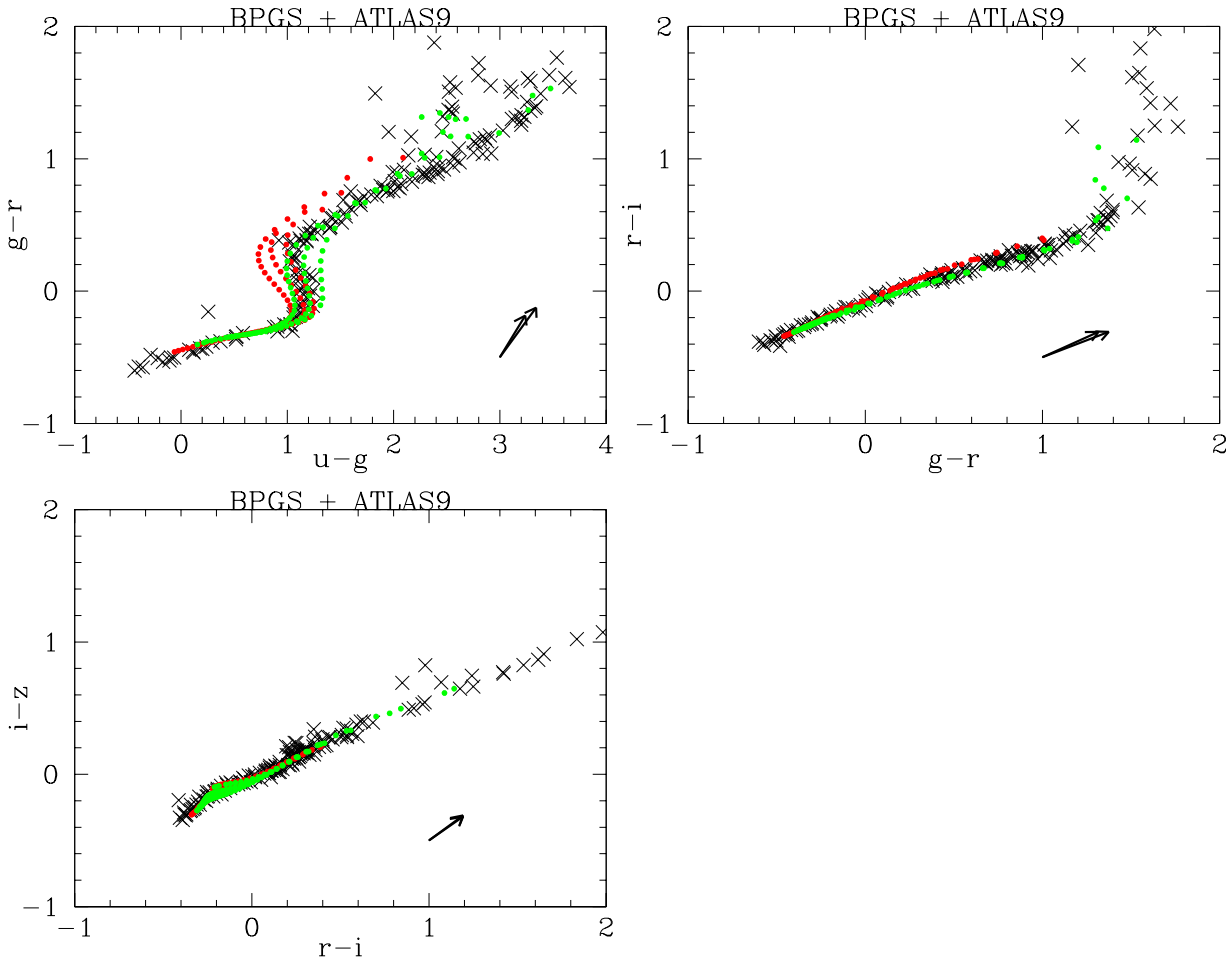


Fig. 14. Color-color diagrams in SDSS AB magnitude. The crosses are synthetic colors calculated from BPGS SEDs. The filled red circles are $[\text{Fe}/\text{H}]=-2.5$ with $[\alpha/\text{Fe}]=+0.4$ models, and the filled green circles are $[\text{Fe}/\text{H}]=0$ with $[\alpha/\text{Fe}]=0$ models. Models are calculated from the flux data of ATLAS9 grid, and the sets of the temperature and the surface gravity are taken from Yonsei-Yale isochrone. The arrows indicate the direction of $A_V=1$ reddening of Galactic extinction for O and M stars in BPGS.

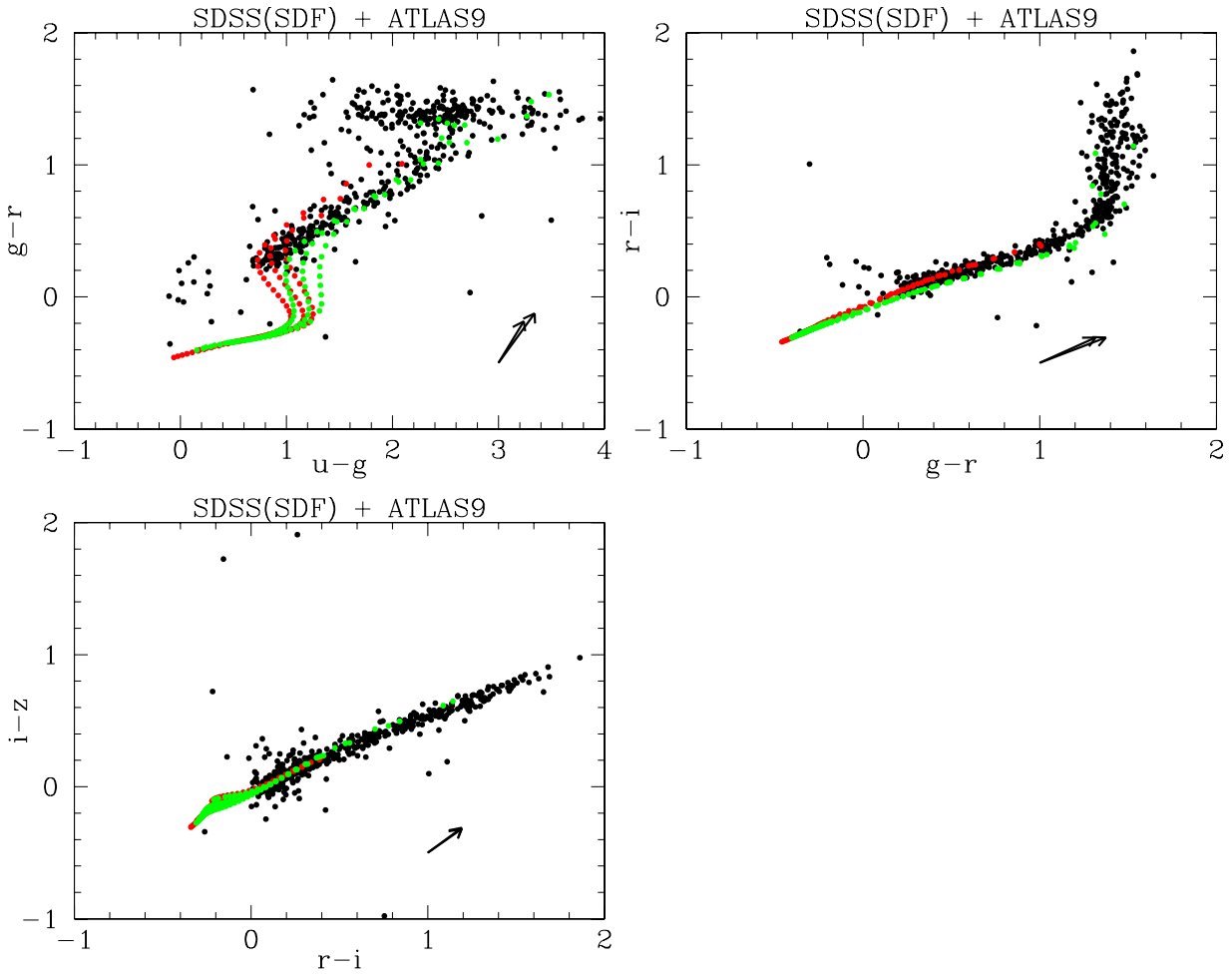


Fig. 15. Same as figure 14, but on SDSS stars. The filled black circles are SDF stars of $15 < r < 21$ taken from SDSS DR8, and are corrected the offset adopted in Kcorrect(Blanton & Roweis 2007) v4.

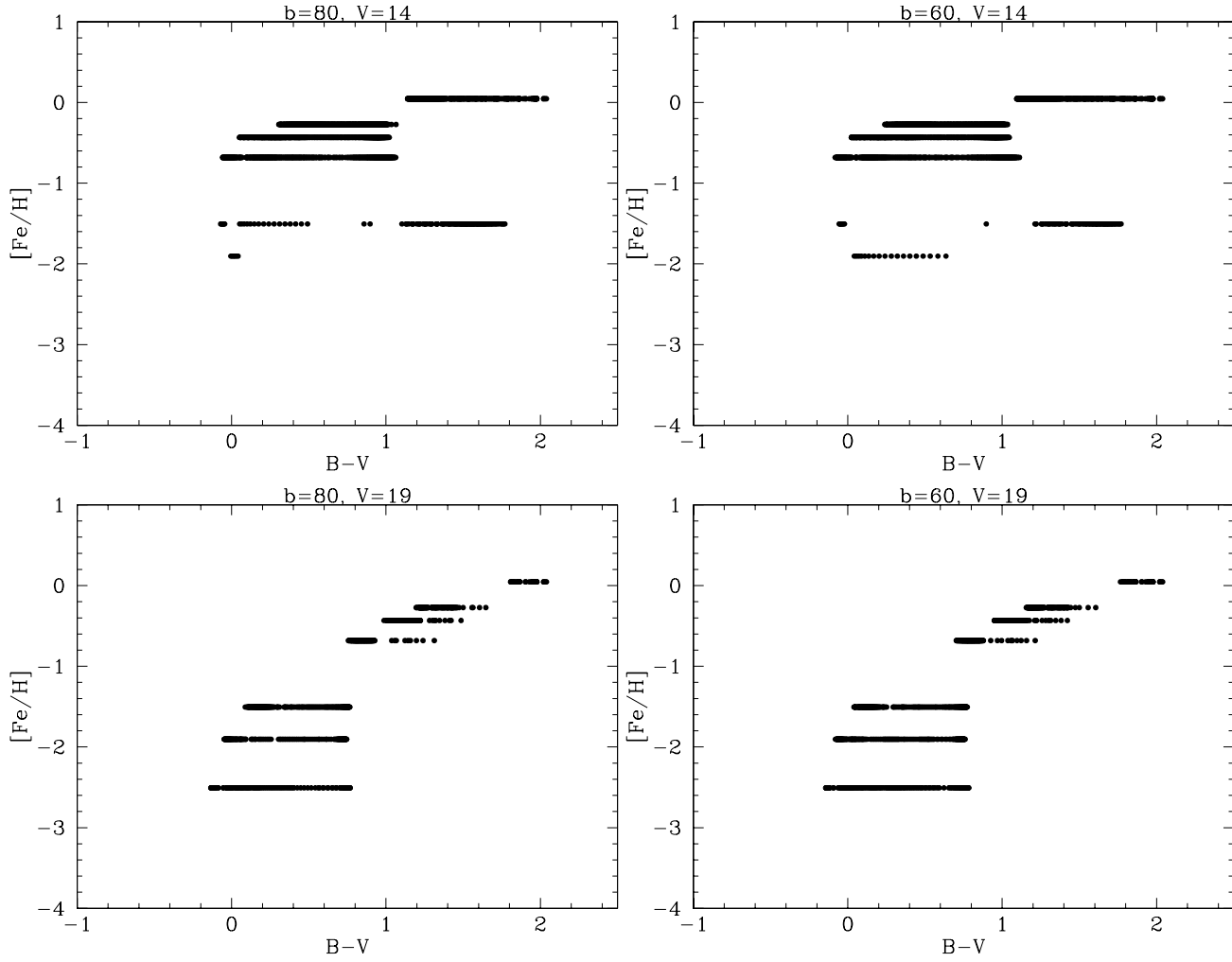


Fig. 16. An estimation of the relation of color and metallicity. (Top left) $V=14$ mag stars at Galactic latitude $b=80$ model. (Top right) $V=14$ mag stars at $b=60$. (Bottom left) $V=19$ mag stars at $b=80$. (Bottom right) $V=19$ mag stars at $b=60$. The metallicity gradient model is taken from Peng, Du, & Wu (2012), and the color-magnitude combination is taken from Y^2 isochrones.

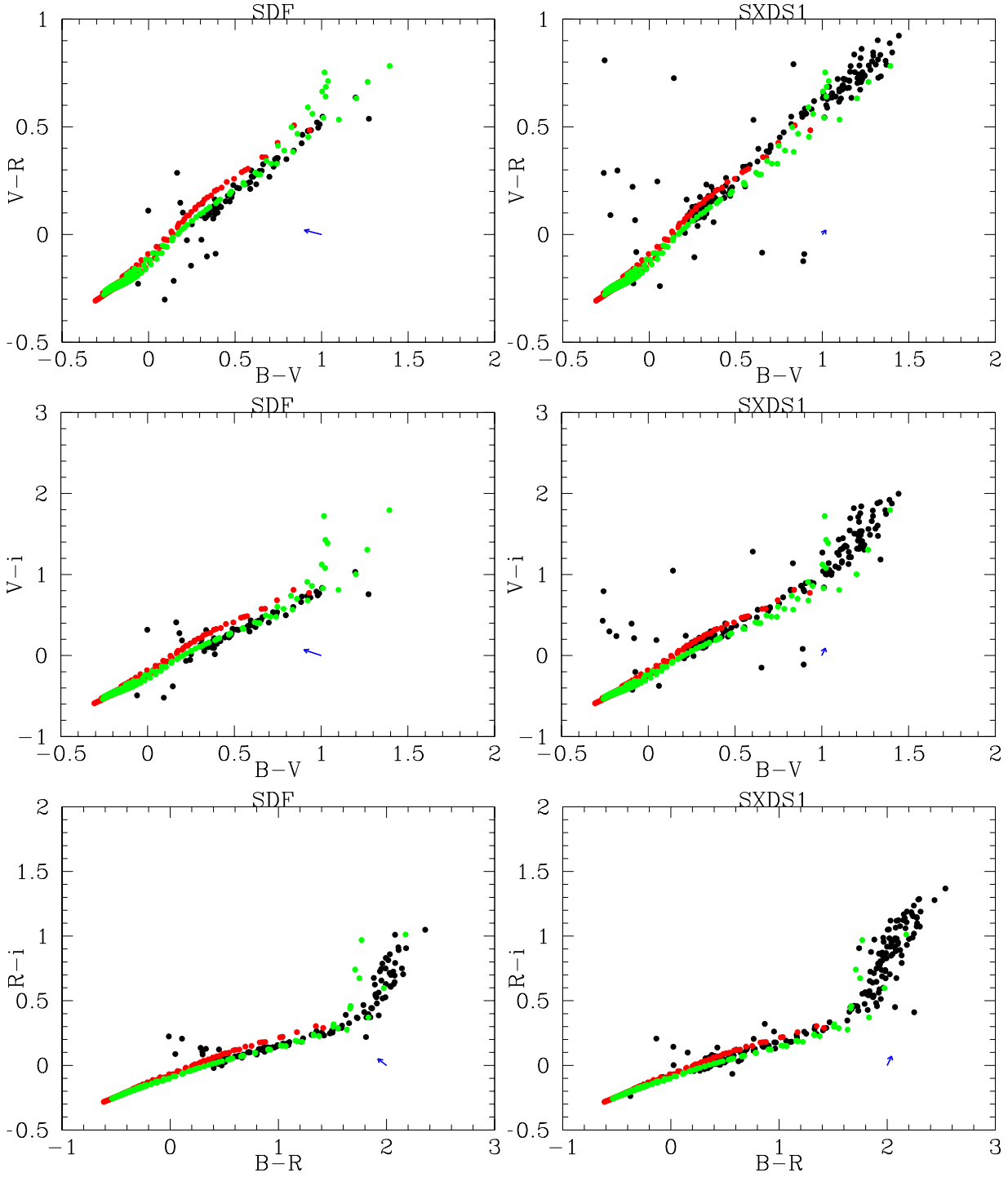


Fig. 17. Color-color diagram of stars in the SDF/SXDS public catalogs which match SDSS. The magnitude ranges are $20.5 < g < 21.5$ for (X-V) vs (V-Y), $20 < r < 21$ for (X-R) vs (R-Y), and $19.5 < i < 20.5$ for (X-i) vs (i-Y), where X=(B,V,R) and Y=(R,i,z). The filled circles are the values in the original SDF/SXDS catalog, and the blue arrow shows our estimation of the offset. The red and green dots are synthetic colors of $[\text{Fe}/\text{H}]=-2.5a$ and $[\text{Fe}/\text{H}]=0$ models, respectively.

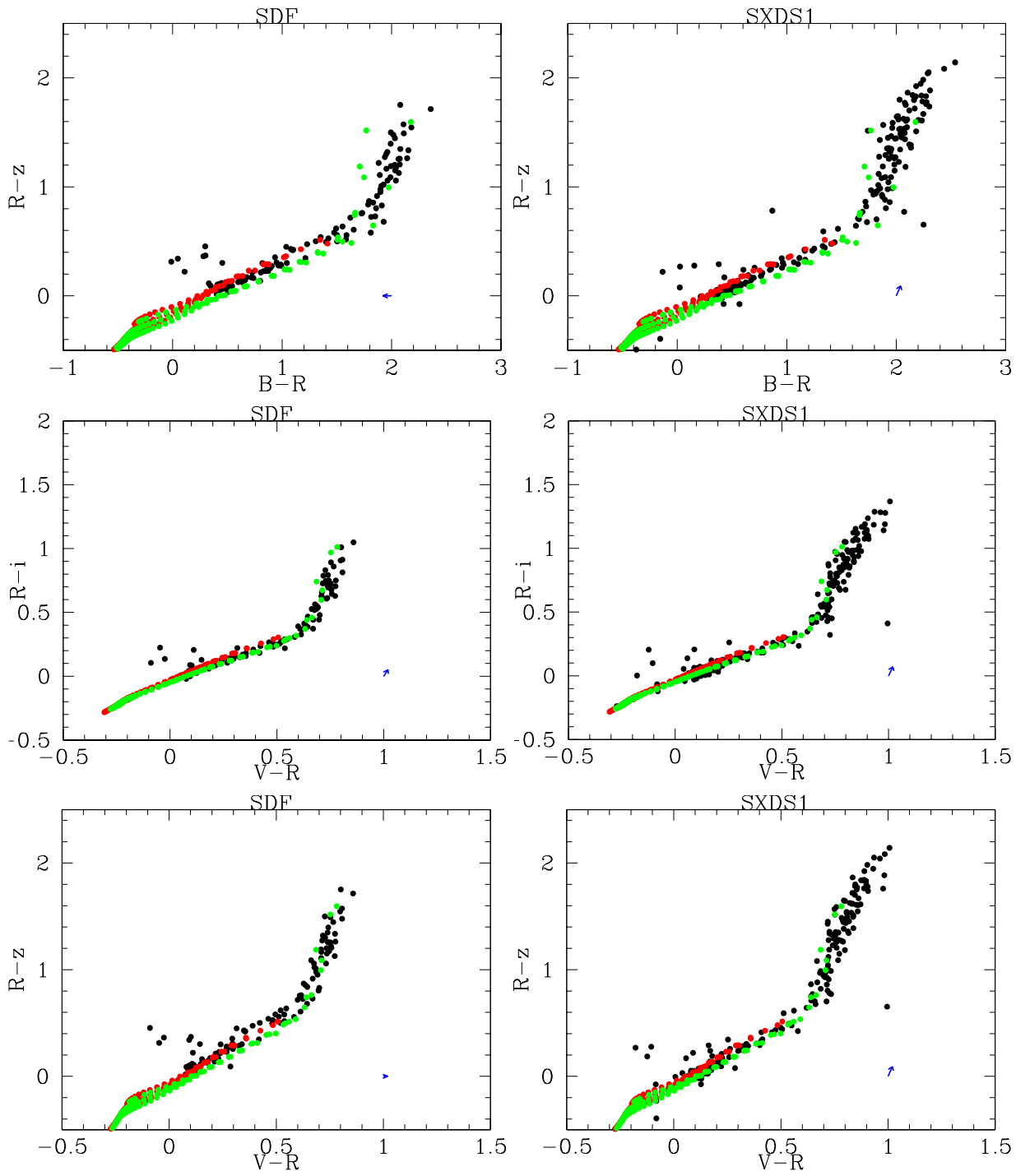


Fig. 17. Continued...

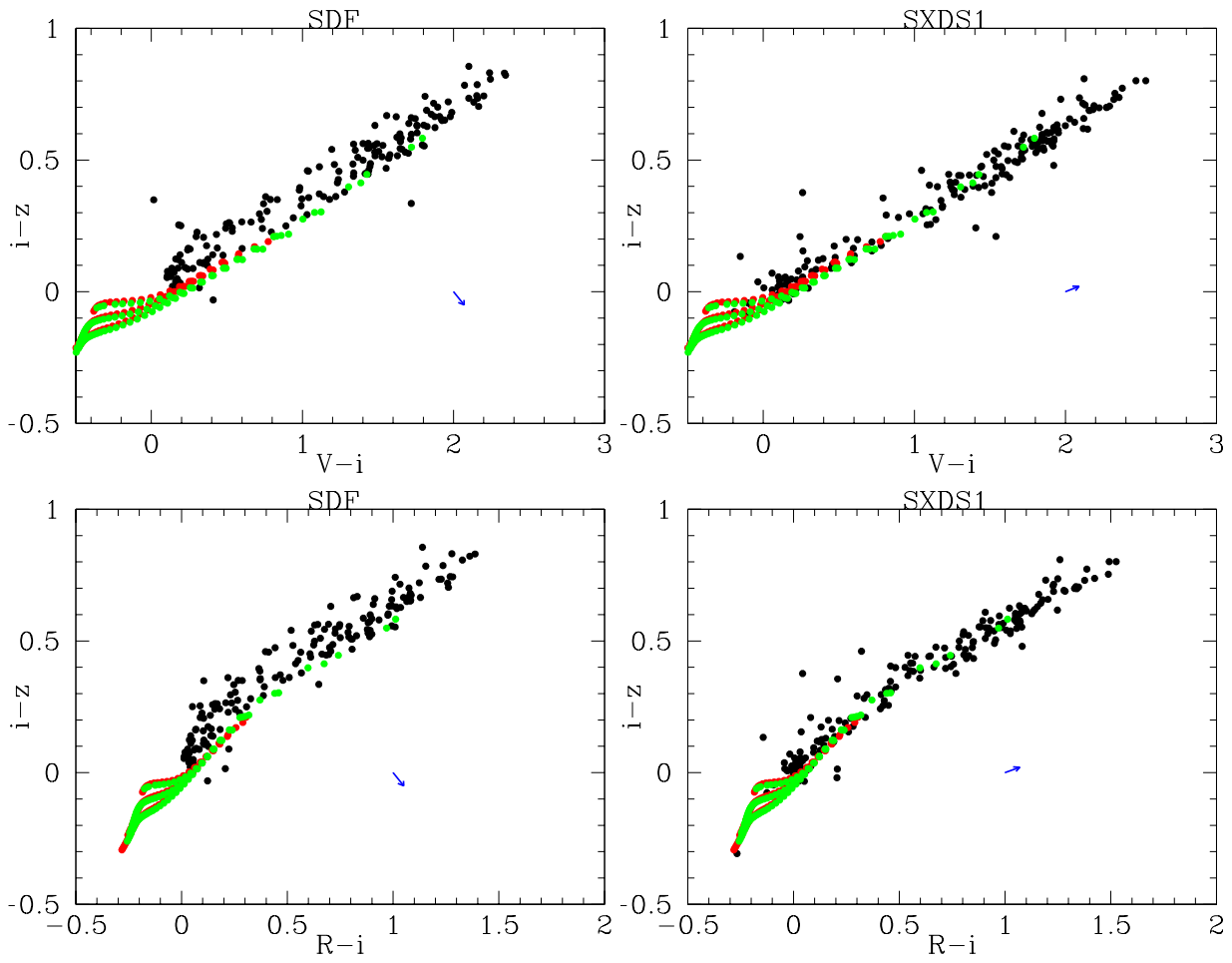


Fig. 17. Continued.

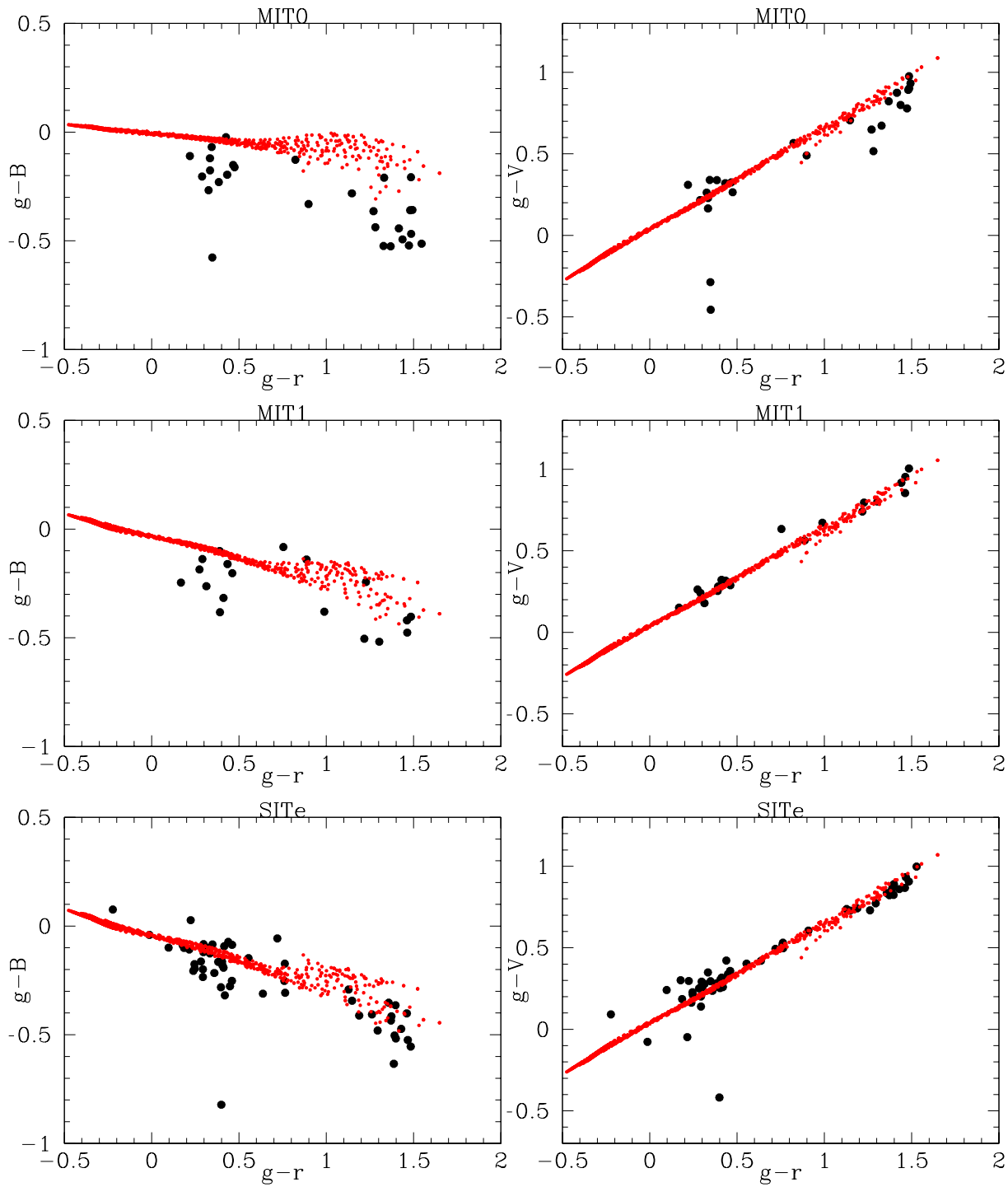


Fig. 18. SDSS color versus the (SDSS)-(Suprime-Cam) color of GT-SXDF-catalog data used in SXDS calibration. The filled red circles represents model colors. In R-band figures, MIT1 model is overplotted, though the difference is indistinguishable.

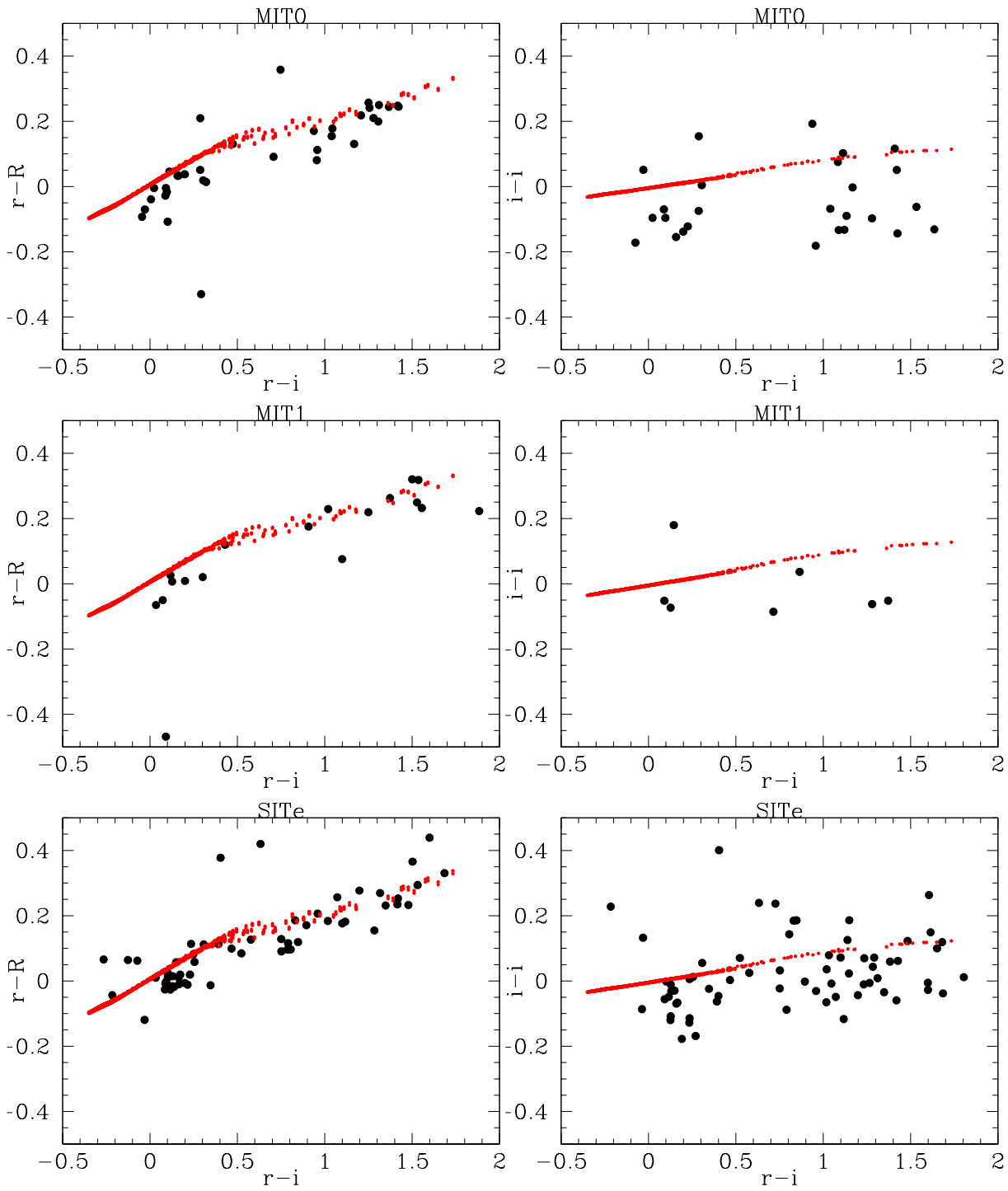


Fig. 18. Continued...

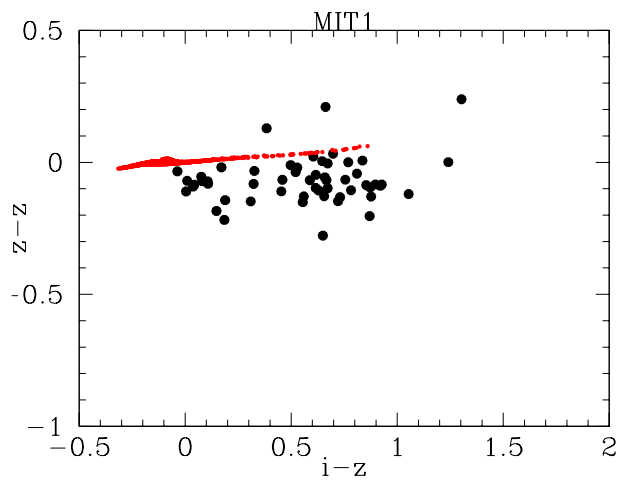


Fig. 18. Continued...

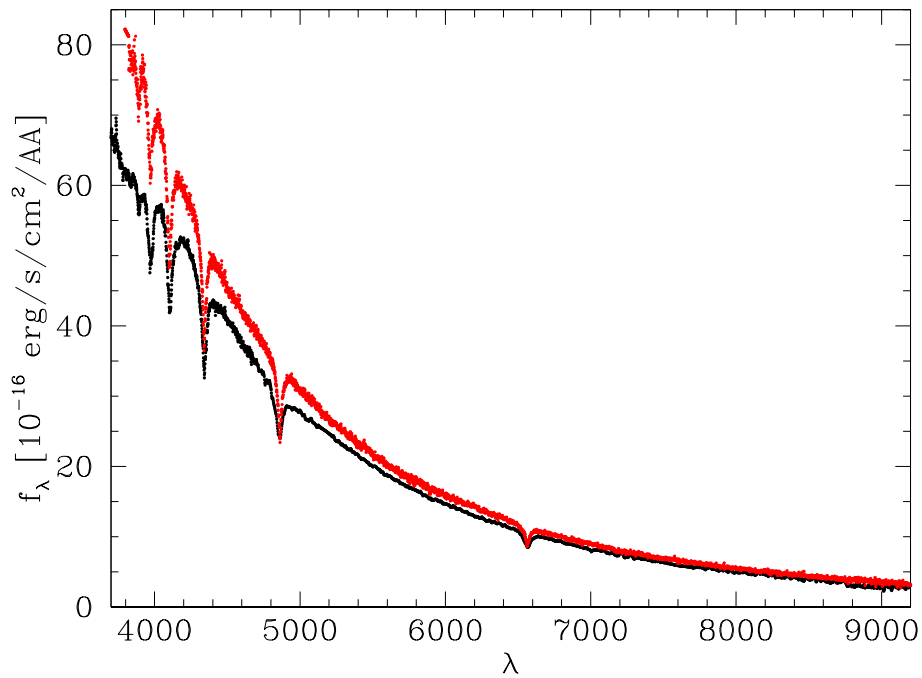


Fig. 19. Spectrophotometric spectra of SA95-42, Black dots are taken from Oke (1990), and red dots are taken from SDSS DR8.

field	R.A.(J2000)	Dec(J2000)
SDF	13 ^h 24 ^m 38 ^s .9	+27°29′25″.9
SXDS-C	02 ^h 18 ^m 00 ^s :00	-05°00′00″.0
SXDS-N	02 ^h 18 ^m 00 ^s :00	-04°35′00″.0
SXDS-S	02 ^h 18 ^m 00 ^s :00	-05°25′00″.0
SXDS-E	02 ^h 19 ^m 47 ^s :07	-05°00′00″.0
SXDS-W	02 ^h 16 ^m 12 ^s :93	-05°00′00″.0

Table 1. Center Position of SDF and SXDS (from Kashikawa et al. 2004; Furusawa et al. 2008)

SDSS-Suprime	SDSS color	range	c_0	c_1	c_2	c_3	c_4	c_5	c_6	c_7
$g - B$	$g - r$	$-0.4 < g - r < 0.7$	-0.037	-0.160	0.009	-0.307	0.246	—	—	—
$g - V$	$g - r$	$-0.4 < g - r < 0.8$	0.038	0.565	-0.024	0.260	-0.218	—	—	—
$r - R$	$r - i$	$-0.4 < r - i < 0.6$	0.006	0.317	-0.065	-0.157	1.667	-1.179	-8.202	9.857
$i - i$	$r - i$	$-0.4 < r - i < 0.8$	-0.005	0.087	0.006	0.011	0.020	-0.015	—	—
$z - z$	$i - z$	$0 < i - z < 0.9$	-0.001	0.092	-0.116	0.109	—	—	—	—

Table 2. The coefficients of best-fit color conversion polynomials

field	B	V	R	i	z
SDF	1.05	1.25	1.33	1.36	1.32
SXDS-C	1.13	1.31	1.27	1.37	1.44
SXDS-N	1.24	1.26	1.35	1.41	1.42
SXDS-S	1.19	1.32	1.33	1.37	1.52
SXDS-E	1.25	1.24	1.42	1.61	1.38
SXDS-W	1.18	1.50	1.59	1.50	1.46

Table 3. The exposure time weighted mean of airmass

band	k_1	k_2	color
B	0.188	-0.016	g-r
V	0.110	-0.001	g-r
R	0.070	-0.000	r-i
i	0.068	0.000	r-i
z	0.102	0.008	i-z

Table 4. The atmospheric extinction coefficients

field	band	N	median	σ	σ_{SDSS}
SDF	B	55	-0.14	0.07	0.03
SDF	V	58	-0.04	0.05	0.03
SDF	R	80	-0.06	0.04	0.03
SDF	i	85	-0.11	0.07	0.03
SDF	z	167	-0.06	0.07	0.05
SXDS-C	B	102	0.00	0.08	0.05
SXDS-C	V	106	-0.02	0.04	0.05
SXDS-C	R	117	-0.04	0.05	0.04
SXDS-C	i	95	-0.11	0.06	0.04
SXDS-C	z	152	-0.13	0.08	0.06
SXDS-N	B	99	0.02	0.07	0.05
SXDS-N	V	101	-0.02	0.06	0.05
SXDS-N	R	113	-0.05	0.05	0.04
SXDS-N	i	89	-0.11	0.06	0.04
SXDS-N	z	146	-0.14	0.08	0.07
SXDS-S	B	65	-0.02	0.08	0.04
SXDS-S	V	67	-0.02	0.04	0.04
SXDS-S	R	81	-0.05	0.04	0.03
SXDS-S	i	70	-0.14	0.08	0.03
SXDS-S	z	121	-0.11	0.07	0.05
SXDS-E	B	98	0.00	0.08	0.05
SXDS-E	V	103	0.00	0.05	0.05
SXDS-E	R	122	-0.04	0.06	0.04
SXDS-E	i	105	-0.13	0.07	0.04
SXDS-E	z	127	-0.15	0.11	0.07
SXDS-W	B	99	-0.01	0.09	0.05
SXDS-W	V	102	-0.03	0.06	0.05
SXDS-W	R	116	-0.05	0.05	0.04
SXDS-W	i	103	-0.08	0.05	0.04
SXDS-W	z	148	-0.14	0.09	0.07

Table 5. The ZP difference between the catalog and the estimated value from SDSS. Difference larger than σ is shown as bold.

star	DR8 objID	$i_{\text{cat}} - i_{\text{syn}}$	$z_{\text{cat}} - z_{\text{syn}}$	SED name
HZ21	1237665330925535274	0.034 \pm 0.016	0.035 \pm 0.020	hz21_001, hz21_002
		-0.002 \pm 0.016	0.018 \pm 0.020	hz21_003
HZ44	1237664672717865012	-0.012 \pm 0.000	0.074 \pm 0.022	hz44_001, hz44_002
		-0.014 \pm 0.000	0.044 \pm 0.022	hz44_003
GD153	1237667735049470025	0.141 \pm 0.001	0.004 \pm 0.021	gd153_mod_002
		0.143 \pm 0.001	0.006 \pm 0.021	gd153_mod_003
		0.136 \pm 0.001	-0.001 \pm 0.021	gd153_mod_004
		0.132 \pm 0.001	-0.005 \pm 0.021	gd153_mod_005
P177D	1237655464320237608	0.005 \pm 0.001	0.017 \pm 0.022	p177d_001
		0.007 \pm 0.001	0.027 \pm 0.022	p177d_stisnic_001
		0.002 \pm 0.001	0.023 \pm 0.022	p177d_stisnic_002
P330E	1237662505371303976	0.008 \pm 0.000	-0.002 \pm 0.015	p330e_001
		0.019 \pm 0.000	-0.031 \pm 0.015	p330e_stisnic_002
		0.015 \pm 0.000	-0.026 \pm 0.015	p330e_stisnic_002

Table 6. Difference between SDSS DR8 catalog magnitude and the synthetic magnitude of standard stars used for SDF